



HAL
open science

Helicity in turbulence modelling by homogenization

Tomas Chacon-Rebollo, Daniel Franco Coronil, F.O. Gallego

► **To cite this version:**

Tomas Chacon-Rebollo, Daniel Franco Coronil, F.O. Gallego. Helicity in turbulence modelling by homogenization. [Research Report] RR-1486, INRIA. 1991. inria-00075076

HAL Id: inria-00075076

<https://inria.hal.science/inria-00075076>

Submitted on 24 May 2006

HAL is a multi-disciplinary open access archive for the deposit and dissemination of scientific research documents, whether they are published or not. The documents may come from teaching and research institutions in France or abroad, or from public or private research centers.

L'archive ouverte pluridisciplinaire **HAL**, est destinée au dépôt et à la diffusion de documents scientifiques de niveau recherche, publiés ou non, émanant des établissements d'enseignement et de recherche français ou étrangers, des laboratoires publics ou privés.

Rapports de Recherche

N° 1486

*Programme 6
Calcul Scientifique, Modélisation et
Logiciels numériques*

**HELICITY IN TURBULENCE
MODELLING BY HOMOGENIZATION**

**Tomas CHACON REBOLLO
Daniel Franco CORONIL
Francisco Ortegon GALLEGO**

Septembre 1991



★ R R . 1 4 8 6 ★

Helicity in Turbulence Modelling by Homogenization

Tomas Chacón Rebollo,* Daniel Franco Coronil,*
& Francisco Ortegón Gallego*

Abstract :

The purpose of this paper is to present a contribution to the mathematical modelling of turbulent flows. A deterministic model for locally homogeneous flows with two spatial scales, obtained by means of homogenization techniques, is derived at first. This is a two-model equations concerning mean turbulent kinetic energy and helicity. The dependence of closure terms on these two parameters is obtained analytically.

An analysis of the physical characteristics of the model is done next. The model is shown to predict a transient oscillatory character of the interactions large-small structures. The mean turbulent helicity is found to act as an agent driving the viscous effects from the small structures to the mean flow, in the sense that the mean flow is affected by the mean turbulent helicity only when the turbulent perturbation lies on the Kolmogorov's viscous subrange. Also, the model is shown to be frame-invariant when the initial perturbation is locally isotropic.

Some numerical tests of our model in the case of 3D Poiseuille flow are finally presented. We compare the results of the model with those furnished by direct numerical solution of Navier-Stokes equations. A good agreement in the behaviour of both turbulent kinetic energy and helicity is found, for the rate of decay and transient effects.

Keywords : Turbulence, separation of scales, homogenization, numerical simulation.

Sur le Rôle de l'Hélicité dans la Modélisation de la Turbulence par Homogénéisation

Résumé :

Ce rapport présente une contribution à la modélisation mathématique des écoulements turbulents. En premier lieu, on dérive un modèle déterministe pour des écoulements homogènes à deux échelles en espace, en utilisant les techniques de l'homogénéisation. Il s'agit d'un modèle à deux équations, qui concerne l'énergie cinétique turbulente et l'hélicité turbulente moyennes.

Ensuite, on développe une analyse des caractéristiques physiques du modèle. On montre que le modèle prédit un comportement oscillatoire de l'évolution des interactions petites-grandes échelles. On montre aussi que l'hélicité turbulente est un agent qui conduit les effets de dissipation visqueuse des petites structures vers l'écoulement moyen, dans le sens que l'hélicité moyenne a un effet sur l'écoulement moyen seulement lorsque la perturbation turbulente git sur le sous-rang visqueux de Kolmogorov. De plus, on démontre que le modèle est invariant par changement de repère si la perturbation initiale est localement isotrope.

Finalement, on présente quelques tests numériques du modèle dans le cas d'écoulements de Poiseuille 3D. On compare les résultats donnés par la résolution numérique du modèle avec ceux donnés par la simulation numérique directe des équations de Navier-Stokes. On trouve un accord acceptable entre ces deux simulations, en ce qui concerne l'évolution des taux de dissipation et les effets transitoires de l'énergie cinétique et aussi de l'hélicité turbulente.

Mots-clés : Turbulence, séparation d'échelles, homogénéisation, simulation numérique.

* Departamento de Análisis Matemático. Facultad de Matemáticas. 41012 Sevilla, Spain. La recherche concernant ce travail a été réalisée en partie lors des visites des deux premiers auteurs à l'INRIA dans le cours des années 1987 à 1990.

0 Introduction

The purpose of this paper is to present a contribution to the analysis of the behaviour of incompressible viscous flows. It is known that these flows are governed by the Navier-Stokes equations; we shall consider here an adimensional form, in the whole space \mathbb{R}^3 :

$$\left. \begin{aligned} u_{,t} + (u \cdot \nabla)u - \frac{1}{\Re} \Delta u + \nabla p = 0; \quad \nabla \cdot u = 0 & \quad \text{in } \mathbb{R}^3 \times]0, T[, \\ u(x, 0) = u_0(x) & \quad \text{in } \mathbb{R}^3. \end{aligned} \right\} \quad (1)$$

Here, $u(x, t)$, $p(x, t)$ are the velocity and pressure at the point $x \in \mathbb{R}^3$ and time t ; $\Re > 0$ is the Reynolds number, u_0 is the initial velocity and T is the final time of the experiment. Under regularity hypotheses on u_0 , this problem, completed with suitable conditions at infinity, has at least a global weak solution. Moreover, this solution is unique, if it is smooth enough and T is not too large. (cf. [4, 15, 18, 30]).

It is also well known that solving numerically problem (1) becomes an unfeasible task in most of the cases of practical interest. Indeed, it is estimated that the smallest structures created in the flow have a size of order $\Re^{-2/4}$ (see ([14])). Thus, an accurate simulation of (1) in the cases of interest ($\Re \geq 10^3$) would require millions of mesh points. However, in most cases only certain average characteristic magnitudes of the flow are needed (for instance, total drag of a car, mean lift of a wing, etc.). This gives rise to the idea of turbulence modelling: How to obtain effective equations that govern the mean values of the flow.

Due to the highly chaotic and unstable behaviour of turbulent flows, it is customary in turbulence modelling to consider the flow field $u(x, t)$ as a random process for each $x \in \mathbb{R}^3$, $t \in [0, T]$. This may be formulated in mathematical terms as follows: If we replace the initial condition $u_0(x)$ in (1) by $\bar{u}_0(x) + u'_0(x, w)$, where $u'_0(x, w)$ is the realization of a random process with known distribution function and zero mean, then the solution (u, p) of (1) is also random. Indeed, equation (1) provides a deterministic mechanism to drive the initial flow to the actual flow at time t .

Once the distribution functions of u and p are known, it is possible to obtain some information about the mean flow, starting from the system (1). For instance, averaging the two equations of (1) we obtain the so-called Reynolds equations for the mean velocity \bar{u} and the mean pressure \bar{p} :

$$\bar{u}_{,t} + (\bar{u} \cdot \nabla)\bar{u} - \nu \Delta \bar{u} + \nabla \bar{p} = -\nabla \cdot \overline{u' \otimes u'}; \quad \nabla \cdot \bar{u} = 0 \quad \text{in } \mathbb{R}^3 \times]0, T[. \quad (2)$$

Here, u' represents the "turbulent perturbation" or "fluctuation", defined by

$$u' = u - \bar{u}.$$

Solving system (2), sets a “closure problem”: How to express the tensor $\overline{u' \otimes u'}$ (called Reynolds tensor) in terms of \bar{u} and \bar{p} . This is the essential problem in turbulence modelling which has received only partial answers up to day. Note that in particular the obtention of the distribution function of $u' \otimes u'$ is almost always impossible, for even the one of u is usually unknown.

A classical way of attempting to solve Reynold’s problem relies on the physics of fluid flows. Experimental measurements show that $\overline{u' \otimes u'}$ is in many cases parallel to $\nabla \bar{u} + \nabla \bar{u}^T$ (Boussinesq’s Hypothesis). Thus we may write

$$\overline{u' \otimes u'} = -\nu_t(\nabla \bar{u} + \nabla \bar{u}^T), \quad (3)$$

where ν_t is the so-called coefficient of “eddy viscosity”, assumed to be positive. In the well known $k - \epsilon$ turbulent model, ν_t is given by means of dimensional analysis as

$$\nu_t = \mu \frac{k^2}{e}$$

where μ is a numerical universal constant (to be obtained from experimental results), k is the kinetic turbulent energy and e is the rate of viscous dissipation of turbulence, defined by (cf. [16, 26]):

$$k = \frac{1}{2} \overline{|u'|^2}, \quad e = \frac{\nu}{2} \overline{|\nabla u' + \nabla u'^T|^2}.$$

Transport equations for k and e are provided in order to close the problem.

Classical models of turbulence are extensively used in practice, in particular in industrial applications. However, they may fail to give correct predictions of the flow, as soon as the physical hypotheses upon which they are based are not true. In addition, it is not clear under which conditions this would happen, as a consequence of the lack of a rigorous definition of average operators.

The purpose of this paper is to develop a model for a class of turbulent flows, that will give a mathematically rigorous definition of averaging and will make apparent clear conditions of applicability. Our derivation is based upon the work of MacLaughlin, Papanicolaou, Pironneau. In [19] these authors introduce a model of turbulence for flows in two spatial scales, which was the object of study of many later works ([2, 3, 5, 6, 7, 8, 22, 23, 24]). We shall refer to these models as “MPP models”.

In this work, we shall consider initial conditions in (1) of the form

$$u(x, 0) = u_0(x) + \epsilon^{1/3} w^0 \left(\frac{x}{\epsilon}, x \right), \quad (4)$$

where $\epsilon > 0$ is an small parameter, u_0 is a smooth vector field on \mathbb{R}^3 , and $w^0(y, x)$ is a smooth vector field on $\mathbb{R}^3 \times \mathbb{R}^3$. w^0 is assumed to be almost-periodic in the y -variable,

for each $x \in \mathbb{R}^3$, and to have zero mean; defined as follows:

$$\langle w^0 \rangle = \langle w^0 \rangle (x) = \lim_{R \rightarrow \infty} \frac{\int_{B_R} w^0(y, x) dy}{\int_{B_R} dy}, \quad (5)$$

where B_R is the closed ball of \mathbb{R}^3 of center the origin and radius R .

This formalism provides a deterministic way of averaging in the framework of almost-periodic functions, and then, of defining mean flow and turbulent perturbation. Now, u_0 can be regarded as the initial mean velocity and $\epsilon^{1/3} w^0$ as the initial perturbation.

In the preceeding MPP models, the initial perturbation w^0 was assumed to be periodic in the y variable. The heart of this paper is to show that the same model is still obtained if w^0 is almost-periodic in the y -variable. This will lead to some improvements of the model and, in particular, to clarify the role of the mean helicity of the fluctuation.

This paper is organized as follows:

In sections 1 to 5 we show that the derivation of [19] still holds in the framework of almost-periodic functions. This leads to a two-equations model concerning mean kinetic energy (q) and helicity (h) of the perturbation u' , an approximation ($u + \epsilon^{2/3} \bar{u}^{(1)}$) of order ϵ to the mean flow \bar{u} and the inverse Lagrangian coordinates associated to the velocity field u (a). This model is the following:

$$\left. \begin{aligned} u_{,t} + (u \cdot \nabla)u + \nabla p &= 0, & \nabla \cdot u &= 0 & \text{in } \mathbb{R}^3 \times \mathbb{R}, \\ a_{,t} + (u \cdot \nabla)a &= 0, & a(x, 0) &= x & \text{in } \mathbb{R}^3 \times \mathbb{R}, \\ q_{,t} + (u \cdot \nabla)q + q \left[\mathbf{R}^*(C) : \nabla u + \mu \left(\frac{h}{q} \right)^2 \psi_q^*(C) \right] &= 0, & & & \text{in } \mathbb{R}^3 \times \mathbb{R}, \\ h_{,t} + (u \cdot \nabla)h + h \left[\mathbf{S}^*(C) : \nabla u + \mu \left(\frac{h}{q} \right)^2 \psi_h^*(C) \right] &= 0, & & & \text{in } \mathbb{R}^3 \times \mathbb{R}, \\ \bar{u}_{,t}^{(1)} + (u \cdot \nabla)\bar{u}^{(1)} + (\bar{u}^{(1)} \cdot \nabla)u + \nabla \bar{p}^{(1)} + \nabla \cdot (q \mathbf{R}^*(C)) &= 0, & \nabla \cdot \bar{u}^{(1)} &= 0 & \text{in } \mathbb{R}^3 \times \mathbb{R}, \end{aligned} \right\} (6)$$

with $G = \nabla a$, $C = G^t G$.

Here, \mathbf{R}^* , \mathbf{S}^* are 3×3 tensors and ψ_q^* , ψ_h^* are scalar functions. These are the closure terms of our model. They depend only on the mean velocity field, by means of a "universal" fluctuation \tilde{w}^* , that verifies an universal "microstructure" problem, that includes a generalized Euler equation for \tilde{w}^* :

$$\left. \begin{aligned} \tilde{w}_{,\tau}^* + (\tilde{w}^* \cdot \nabla_y)\tilde{w}^* + (C \nabla_y)\pi^* &= 0, & \nabla_y \cdot \tilde{w}^* &= 0 & \text{in } \mathbb{R}^3 \times \mathbb{R} \\ \tilde{w}^*(y, 0) &= \frac{1}{\sqrt{q_0}} w^0 \left(\frac{q_0}{h_0} y \right), & & & \text{in } \mathbb{R}^3 \\ \tilde{w}^*, \pi^* & \text{almost-periodic in } (y - \tau). \end{aligned} \right\} (7)$$

Here, π^* is the pressure associated to \tilde{w}^* . Also, q_0 and h_0 are the mean kinetic energy and the helicity of the initial perturbation w^0 , respectively, assumed to be nonzero.

In Section 6 we analyze the connexions of model (6) with the classical models of turbulence. Model (6) is regarded as a two-equations model for locally homogeneous turbulence in Kolmogorov's equilibrium range. Some numerical experiments included in this paper, together with other previous works about MPP models are analyzed, in order to show that model (6) takes into account a transient oscillatory character of the interaction large-small structures, which usual models of turbulence are unable to reproduce. However, it is found to need further improvements to predict eddy diffusion effects, as all preceding MPP models. Moreover, we analyze the role of the mean helicity of the microstructures h , a statistic of the turbulent perturbation which is present in our model, but which is usually absent of the classical models of turbulence. The helicity appears as an agent that drives the viscous effects from the small scales to the mean flow in the sense that it affects the mean flow only if the turbulent perturbation lies on the viscous subrange. If the perturbation lies on the inertial subrange, the helicity is shown to become a passive agent.

In Section 6 we also show that model (6) reduces in some particular cases to known two-equations models. Concretely, when the initial mean velocity is constant, model (6) is shown to be equivalent to

$$\left. \begin{aligned} q_{,t} + e &= 0, \\ e_{,t} + d \frac{e^2}{q} &= 0, \end{aligned} \right\} \text{ in } \mathbb{R}^3 \times \mathbb{R}; \quad (8)$$

where e is the rate of viscous dissipation of turbulence, and d is a numerical constant. Constant d is (theoretically) computable from the solution of the microstructure problem (7). In the classical theory of isotropic turbulence (developped, for instance, by Reynolds in [27]), model (8) is assumed to apply to well developped locally isotropic turbulence, and is obtained by means of dimensional analysis. Reynolds shows in [27] that some particular solutions of model (8) correspond to perturbations that have an energy spectrum containing the Kolmogorov's law in $k^{-5/3}$ for the inertial range. However, we do not know whether it is possible to prove analytically this result in our case, in the framework of almost-periodic perturbations.

In Section 7 we analyze some properties of physical relevance of our model that occur when the initial perturbation is locally isotropic. A mathematical definition of this concept is given at first: The perturbation w^0 is said to be locally isotropic at a point $x \in \mathbb{R}^3$, if

$$w^0(Qy, x) = Qw^0(y, x) \quad \text{for all rotation matrix } Q, \quad \text{for all } y \in \mathbb{R}^3.$$

We give a mathematical proof that in this case, model (6) is frame-invariant. In [28, 29], Speziale sets some necessary conditions related to frame-invariance, that turbulence models

must verify to be physically consistent, when the frame of reference is non-inertial and inertial. Our model is found to verify these conditions when the frame is non-inertial.

In Section 8 we perform a testing of our model in the case of 3D Poiseuille flow between flat plates with two scales. A model including eddy viscosity terms is tested. We solve numerically the model equations and also the Navier-Stokes equations separately. Our tests consist in comparing suitably the results of both simulations. Concretely, we observe that our model reproduces very accurately the evolution of mean velocity, mean turbulent kinetic energy and helicity as far as there is a significant level of turbulence; and as long as the scales are separated.

Finally, in Section 9 we present some numerical results that show an oscillatory behaviour in the transport of helical microstructures. This kind of behaviour is qualitatively explained by means of our model equations, in the absence of diffusion effects; as in the case of nonhelical microstructures.

As a conclusion, we can say that this paper presents a version of the MPP model of turbulence that applies to almost-periodic perturbations. From the point of view of turbulence modelling by homogenization, it provides some improvements to former MPP models: The expressions of the structures of the closure terms are simplified, and the role of the helicity is clarified. From the point of view of "classical" turbulence modelling, we propose a two-equations model which takes into account some transient oscillatory effects in the interaction large-small structures, and which includes in a natural way the mean helicity of the perturbation, as one of the two statistics of the model. The mean helicity of the microstructures is shown to act as an agent driving the viscous effects to the mean flow. Numerical experiments for genuine 3D flows are presented, that support the validity of the model.

1 Statement of the problem

In Sections 1 to 5 we shall develop a new version of the model for convection of microstructures introduced in [19] by McLaughlin, Papanicolaou & Pironneau. This version will apply to slightly viscous flows with initialization in two scales. Our purpose is to apply the techniques introduced in [19] to the obtention of a model for locally homogeneous turbulence, in the framework of almost-periodic perturbations.

Let $\epsilon > 0$ be a small parameter and $T > 0$ a given final time. We shall consider the Navier-Stokes equations for three-dimensional viscous fluids in $\mathbb{R}^3 \times]0, T[$; with kinematic viscosity of order ϵ^2 :

$$u^\epsilon_t + (u^\epsilon \cdot \nabla)u^\epsilon + \nabla p^\epsilon - \mu \epsilon^2 \Delta u^\epsilon = 0, \quad \nabla \cdot u^\epsilon = 0 \quad \text{in } \mathbb{R}^3 \times]0, T[. \quad (9)$$

Here, $u^\epsilon(x, t)$ and $p^\epsilon(x, t)$ are the velocity and pressure fields, respectively, and $\mu > 0$ is a given number of order one. We wish to analyze the time evolution of flows with initial data of the form

$$u^\epsilon(x, 0) = u_0(x) + \epsilon^{1/3} w^0\left(\frac{x}{\epsilon}, x\right) \quad \text{in } \mathbb{R}^3, \quad (10)$$

where u_0 is a smooth velocity field in \mathbb{R}^3 and $w^0(y, x)$ is a smooth velocity field in $\mathbb{R}^3 \times \mathbb{R}$. Note that ϵ represents the dimensionless ratio of characteristic length scales associated to the initial data $u^\epsilon(x, 0)$. It is known that problem (9)-(10), completed with suitable conditions at infinity, has a unique smooth solution if T is not too large (cf. [4, 15, 18, 30]).

In [19] and later works, MPP models have been developed by assuming that $w^0(\cdot, x)$ is periodic with zero mean on a period cell, for all $x \in \mathbb{R}^3$. Then, the highly oscillating velocity field $\epsilon^{1/3} w^0(\frac{x}{\epsilon}, x)$ can be regarded as the initial "turbulent" perturbation, and the field $u_0(x)$ as the initial "mean" velocity. Our purpose here is to show that the derivation of [19] still holds if $w^0(\cdot, x)$ is almost-periodic in \mathbb{R}^3 , for all $x \in \mathbb{R}^3$. Roughly speaking, almost-periodic functions are characterized by having a discrete Fourier Spectrum (see [12, 31]). From a mathematical point of view, the class of almost-periodic functions can be defined as the closure of all trigonometric polynomials with the uniform norm. Some properties of almost-periodic functions are of interest for our purposes. They are stated as follows:

Theorem 1 : *Assume $v_1, v_2 : \mathbb{R}^3 \rightarrow \mathbb{R}$ are almost-periodic. Then, $\lambda v_1 + \mu v_2, \forall \lambda, \mu \in \mathbb{R}$, and $v_1 \cdot v_2$ are also almost-periodic. ■*

Theorem 2 : *Assume $v : \mathbb{R}^3 \rightarrow \mathbb{R}$ is almost-periodic. Then the following statements hold:*

i) Given $R > 0$, let us denote by B_R the closed ball of \mathbb{R}^3 of radius R and center the origin. Then the mean

$$\langle v \rangle = \lim_{R \rightarrow \infty} \frac{\int_{B_R} v(y) dy}{\int_{B_R} dy} \quad (11)$$

exists.

ii) If $v \geq 0$ and $\langle v \rangle = 0$, then $v = 0$.

iii) Given $z \in \mathbb{R}^3$, denote by v_z the z -translated function of v : $v_z(y) = v(y + z)$. Then,

$$\langle v_z \rangle = \langle v \rangle .$$

iv) Given a rotation matrix Q (i.e., $Q^t = Q^{-1}$, $\det(Q) = 1$) of order 3, denote by v_Q the Q -rotated function of v : $v_Q(y) = v(Qy)$. Then,

$$\langle v_Q \rangle = \langle v \rangle .$$

■

The proof of Theorem 1 can be found, for instance, in [12], and that of Theorem 2 in [13].

In what follows we shall assume $w^0(\cdot, x)$ to be almost-periodic in \mathbb{R}^3 , for all $x \in \mathbb{R}^3$. Furthermore, we shall assume that $w^0(y, x)$ has zero y -mean:

$$\langle w^0 \rangle = \langle w^0 \rangle (x) = 0, \quad \forall x \in \mathbb{R}^3. \quad (12)$$

This formalism allows us to give a mathematically rigorous definition of mean flow and “turbulent” perturbation in our initial conditions (10), in the same way as in [19].

Remarks:

1. Note that the average operator defined in (11) has two well known properties in turbulence modelling: It is homogeneous and isotropic, as a consequence of ii) and iii) in Theorem 2. This means that the initial perturbation is locally homogeneous, in the sense of Batchelor (cf. [1]). However, in general the initial perturbation is not necessarily locally statistically isotropic (see Section 7 for details).
2. Here, we are considering a generalization of the hypotheses on w^0 made in [19]. Indeed, let us assume that a function v is periodic with period cell Y . Then, v is also almost-periodic, and

$$\langle v \rangle = \frac{\int_Y v(y) dy}{\int_Y dy} .$$

3. Let us remark that the choice of orders of magnitude of the initial perturbation in (10) and of the coefficient on viscosity in (9) can be explained in the framework of Kolmogorov's theory of turbulence. In this context, ϵ^2 appears as the highest order of magnitude of viscosity for which a range of eddies of characteristic size ϵ and characteristic velocity $\epsilon^{1/3}$ may exist. An analysis of this fact, and more generally of the connexions of our model with Kolmogorov's theory of turbulence, will be made in Section 6. ■

Our purpose is to obtain a mathematical description of the behaviour of the solution u^ϵ, p^ϵ of (9)-(10) for $t > 0$ when ϵ is small. From the physical point of view, this problem is the analysis of the interaction between a turbulent perturbation in small scale and the mean flow, in the presence of a slight viscous dissipation. We assume the perturbation to exist at $t = 0$, and we wish to know the behaviour of the flow at later times. In practice, this situation occurs in the case of flows with spectral gap, such as flow past a grid, atmospheric flow and others (cf. [25]).

2 Cascade of equations

In this Section, we shall obtain effective equations for the evolution of u^ϵ and p^ϵ by an asymptotic technique, introduced in [19] and applied in [7] to slightly viscous fluids.

We shall assume that u^ϵ, p^ϵ admit asymptotic expansions of the form

$$\begin{aligned} u^\epsilon(x, t) &\sim u(x, t) + \epsilon^{1/3} w\left(\frac{a(x, t)}{\epsilon}, \frac{t}{\epsilon^{2/3}}; x, t\right) + \epsilon^{2/3} u^{(1)}\left(\frac{a(x, t)}{\epsilon}, \frac{t}{\epsilon^{2/3}}; x, t\right) + \\ &\quad + \epsilon u^{(2)}\left(\frac{a(x, t)}{\epsilon}, \frac{t}{\epsilon^{2/3}}; x, t\right) + \dots \\ p^\epsilon(x, t) &\sim p(x, t) + \epsilon^{1/3} p^{(0)}\left(\frac{a(x, t)}{\epsilon}, \frac{t}{\epsilon^{2/3}}; x, t\right) + \epsilon^{2/3} \pi\left(\frac{a(x, t)}{\epsilon}, \frac{t}{\epsilon^{2/3}}; x, t\right) + \\ &\quad + \epsilon p^{(1)}\left(\frac{a(x, t)}{\epsilon}, \frac{t}{\epsilon^{2/3}}; x, t\right) + \dots \end{aligned} \tag{13}$$

Here $a(x, t)$ are the inverse Lagrangian coordinates associated to the velocity u :

$$a_t + (u \cdot \nabla) a = 0, \quad \text{in } \mathbb{R}^3 \times]0, T[; \quad a(x, 0) = x. \tag{14}$$

Also, $w(y, \tau; x, t), u^{(k)}(y, \tau; x, t), \pi(y, \tau; x, t), p^{(k)}(y, \tau; x, t), \forall k \geq 0$, are smooth functions defined on $\mathbb{R}^3 \times \mathbb{R} \times \mathbb{R}^3 \times [0, T]$. We shall assume that all functions $w, u^{(k)}, \pi, p^{(k)}$ are smooth and almost-periodic in the $y - \tau$ variables. In particular, this implies that they are bounded functions in the $y - \tau$ variables for each given $x \in \mathbb{R}^3, t \in [0, T]$ (cf. [12, 31]). This will allow us to distinguish between consecutive terms in the expansions.

Remarks:

1. Due to the almost-periodicity, the $y - \tau$ mean of all terms, defined for instance for w as

$$\ll w \gg (x, t) = \lim_{R \rightarrow \infty, \tau \rightarrow \infty} \frac{\int_{-\tau}^{\tau} \int_{B(R)} w(y, \sigma; x, t) dy d\sigma}{2\tau \int_{B(R)} dy}, \quad (15)$$

exists. This space-time average operator is homogeneous in space and time, and isotropic in space. Note that the calculation of (15) does not involve "integration through the futur" in large scale time t , because the microscale time τ is infinitesimal with respect to the large scale time t . Also, the mean (15) exists for $y - \tau$ periodic functions (see [13]); and if a function v is periodic in y and τ with period cell $Z = Y \times [0, 2\pi]$, then it is almost-periodic in y and τ , and

$$\ll v \gg = \frac{\int_Z v(y, \tau) dy d\tau}{\int_Z dy d\tau}$$

2. The expansion in (13) for the velocity u^ϵ has to be understood in the sense that for all $k \geq 0$, there exists a constant C_k independent of ϵ , such that

$$\|u^\epsilon - S_k^\epsilon\| \leq C_k \epsilon^{(k+1)/3},$$

where

$$S_k^\epsilon(x, t) = u(x, t) + \left[\epsilon^{1/3} w(y, \tau; x, t) + \sum_{l=2}^k \epsilon^{l/3} u^{(l)}(y, \tau; x, t) \right] \Big|_{y=\frac{\alpha(x,t)}{\epsilon}, \tau=\frac{t}{\epsilon^{2/3}}},$$

and $\|\cdot\|$ is a suitable space-time norm. A similar interpretation applies to the expansion in (13) for the pressure p^ϵ .

3. The choice of such a complicated ansatz as (13) is not arbitrary. In particular, the equation verified by function $a(x, t)$ is suggested by the Taylor hypothesis for turbulent flows: The perturbation is transported by the mean flow. Note that $a(x, t)$ is constant along the stream lines associated to the velocity u . Also, it is reasonable to expect that the oscillations in space beared by the initial perturbation, $\epsilon^{1/3} w^0(\frac{x}{\epsilon}, x)$, will produce oscillations in time. Dimensional analysis gives a characteristic size of $\epsilon^{2/3}$ for such oscillations. ■

To obtain formal equations for the terms of expansions (13), at first one has to express equations (9) as expansions in powers of ϵ . In condensed form, these expansions are:

$$\begin{aligned}
& \epsilon^{-2/3}\{(a_{,t} + u \cdot \nabla a) \cdot \nabla_y \tilde{w} + C \nabla_y p^{(0)}\} + J \\
& + \epsilon^{-1/3}\{(a_{,t} + u \cdot \nabla a) \cdot \nabla_y \tilde{u}^{(1)} + E(\tilde{w}, \pi, C)\} + \\
& + \epsilon^0\{(a_{,t} + u \cdot \nabla a) \cdot \nabla_y \tilde{u}^{(2)} + [L(\tilde{u}^{(1)}, p^{(1)}; \tilde{w}, C) - \tilde{f}^{(1)}]\} + \\
& + \epsilon^{1/3}\{(a_{,t} + u \cdot \nabla a) \cdot \nabla_y \tilde{u}^{(3)} + [L(\tilde{u}^{(2)}, p^{(2)}; \tilde{w}, C) - \tilde{f}^{(2)}]\} + \\
& + \epsilon^{2/3}\{(a_{,t} + u \cdot \nabla a) \cdot \nabla_y \tilde{u}^{(4)} + [L(\tilde{u}^{(3)}, p^{(3)}; \tilde{w}, C) - \tilde{f}^{(3)}]\} + \\
& + \epsilon\{(a_{,t} + u \cdot \nabla a) \cdot \nabla_y \tilde{u}^{(5)} + [L(\tilde{u}^{(4)}, p^{(4)}; \tilde{w}, C) - \tilde{f}^{(4)}]\} + \dots \Big|_{y=\frac{a(x,t)}{\epsilon}, \tau=\frac{t}{\epsilon^{2/3}},} = 0
\end{aligned} \tag{16}$$

and

$$\begin{aligned}
& \epsilon^{-2/3}(\nabla_y \cdot \tilde{w}) + \epsilon^{-1/3}(\nabla_y \cdot \tilde{u}^{(1)} - g^{(1)}) + \epsilon^0(\nabla_y \cdot \tilde{u}^{(2)} - g^{(2)}) + \\
& + \epsilon^{1/3}(\nabla_y \cdot \tilde{u}^{(3)} - g^{(3)}) + \epsilon^{2/3}(\nabla_y \cdot \tilde{u}^{(4)} - g^{(4)}) + \dots \Big|_{y=\frac{a(x,t)}{\epsilon}, \tau=\frac{t}{\epsilon^{2/3}},} = 0.
\end{aligned} \tag{17}$$

Here we have used the following notations:

$$C = G^T G, \quad \text{with } G = \nabla a, \quad (\text{i.e., } G_{ij} = \frac{\partial a_j}{\partial x_i}); \tag{18}$$

$$\tilde{w} = G^T w, \quad \tilde{u}^{(k)} = G^T u^{(k)} \quad \forall k \geq 1; \tag{19}$$

$$E(\tilde{w}, \pi; C)J = \tilde{w}_{,\tau} + (\tilde{w} \cdot \nabla_y) \tilde{w} + C \nabla_y \pi; \tag{20}$$

$$L(\tilde{u}^{(k)}, p^{(k)}; \tilde{w}, C) = \tilde{u}_{,\tau}^{(k)} + (\tilde{w} \cdot \nabla_y) \tilde{u}^{(k)} + (\tilde{u}^{(k)} \cdot \nabla_y) \tilde{w} + C \nabla_y p^{(k)}. \tag{21}$$

Also, functions $\tilde{f}^{(1)}, \tilde{f}^{(2)}, \dots, g^{(1)}, g^{(2)}, \dots$ are defined by

$$\begin{aligned}
\tilde{f}^{(1)} &= -G^T [u_{,t} + (u \cdot \nabla) u + \nabla p] \\
\tilde{f}^{(2)} &= -G^T [w_{,t} + (u \cdot \nabla) w + (w \cdot \nabla) u + \nabla p^{(0)} + (\tilde{u}^{(1)} \cdot \nabla_y) u^{(1)} - \\
& \quad - \mu(G \nabla_y) \cdot ((G \nabla_y) w)] \\
\tilde{f}^{(3)} &= -G^T [u_{,t}^{(1)} + (u \cdot \nabla) u^{(1)} + (u^{(1)} \cdot \nabla) u + \nabla \pi + (\tilde{u}^{(1)} \cdot \nabla_y) u^{(2)} + \\
& \quad + (\tilde{u}^{(2)} \cdot \nabla_y) u^{(1)} + (w \cdot \nabla) w - \mu(G \nabla_y) \cdot ((G \nabla_y) u^{(1)})] \\
\tilde{f}^{(4)} &= -G^T [u_{,t}^{(2)} + (u \cdot \nabla) u^{(2)} + (u^{(2)} \cdot \nabla) u + \nabla p^{(1)} + (\tilde{u}^{(2)} \cdot \nabla_y) u^{(2)} + \\
& \quad + (\tilde{u}^{(3)} \cdot \nabla_y) u^{(1)} + (\tilde{u}^{(1)} \cdot \nabla_y) u^{(3)} + (w \cdot \nabla) u^{(1)} + \\
& \quad + (u^{(1)} \cdot \nabla) w - \mu(G \nabla_y) \cdot ((G \nabla_y) u^{(2)})]
\end{aligned} \tag{22}$$

⋮

$$\begin{aligned}
g^{(1)} &= 0 \\
g^{(2)} &= -\nabla \cdot u \\
g^{(3)} &= -\nabla \cdot w \\
g^{(k)} &= \nabla \cdot u^{(k-3)}, \quad \forall k \geq 4
\end{aligned} \tag{23}$$

Now we apply the principle of singular perturbations. Then, the coefficient of each power of ϵ in (16)-(17) must vanish. Further, we apply the homogenization hypothesis of separation of scales. This, together with (14), gives the following “cascade of equations”:

$$G\nabla_y p^{(0)} = 0, \quad \text{in } \mathbb{R}^3 \times \mathbb{R}; \quad (24)$$

$$E(\tilde{w}, \pi; C) = 0; \quad \nabla_y \cdot \tilde{w} = 0 \quad \text{in } \mathbb{R}^3 \times \mathbb{R}; \quad (25)$$

$$L(\tilde{u}^{(k)}, p^{(k)}; \tilde{w}, C) = \tilde{f}^{(k)}, \quad \nabla_y \cdot \tilde{u}^{(k)} = g^{(k)} \quad \text{in } \mathbb{R}^3 \times \mathbb{R} \quad \forall k \geq 1. \quad (26)$$

Remarks:

1. The name of “cascade of equations” is justified because each $\tilde{f}^{(k)}, g^{(k)}$ depends only upon $u, w, u^{(1)}, \dots, u^{(k-1)}$ and $p, p^{(0)}, \pi, \dots, p^{(k-3)}$. Thus, equation (26) represents the effects of all eddies of characteristics velocities $\epsilon^{1/3}, \epsilon^{2/3}, \dots, \epsilon^{k/3}$ on eddies of characteristic velocity $\epsilon^{(k+1)/3}$.
2. The main fluctuation w verifies the Euler-like equations (25), through the transformed fluctuation \tilde{w} , defined in (19). Equations (25) are of the same mathematical nature of standard Euler equations. Indeed, the changement of variable

$$z = G^{-t}y,$$

reduces (25) to standard Euler equations for the variables

$$\hat{w}(z, \tau) = w(y, \tau); \quad \hat{\pi}(z, \tau) = \pi(y, \tau).$$

One could think of obtaining w and π by means of this changement of variable by solving at first Euler equations for \hat{w} and $\hat{\pi}$. However, this would be inconsistent with the asymptotic analysis that we have made, because if we replace the point $y = \frac{a(x,t)}{\epsilon}$ by $z = G^{-t}(x, t)\frac{a(x,t)}{\epsilon}$ in the expansions (13), then the expansions (16) and (17) would be wrong.

An analogous comment applies to the linearized Euler-like equation (26), verified by the higher order fluctuations $u^{(k)}$.

3. Note that equation (16) justifies partially the equation in (14) for the Lagrangian coordinates $a(x, t)$. Note also that the initial condition in (14) is somewhat arbitrary. Indeed, our asymptotics at $t = 0$ imply

$$w\left(\frac{a(x, 0)}{\epsilon}, 0; x, 0\right) = w^0\left(\frac{x}{\epsilon}; x\right)$$

This can hold for all functions w only if $\frac{a(z\epsilon, 0)}{\epsilon}$ is independent of ϵ , and then

$$a(x, 0) = \sum_{j=1}^n x_j \frac{\partial a}{\partial x_j}(x, 0).$$

Consequently, $a(x, 0)$ must be linear in x . The choice made in (14) is due to reasons of consistency of notation. ■

3 Determination of the main perturbation terms

To obtain a mathematical description of the behaviour of u^ϵ and p^ϵ , solution of Navier-Stokes equations (9)-(10), we wish to obtain equations that govern all terms in the asymptotic expansions (13). In this Section we shall propose a system of equations to determine the main perturbation terms (w, π) .

As we have remarked in the preceding Section, reducing equations (25) to standard Euler equations to obtain w and π becomes inconsistent with our asymptotic analysis. For this reason, we shall use equations (25) as they are to obtain w and π . Let us remark also that equations (25) do not determine completely the pair (\tilde{w}, π) . Indeed, suitable initial and boundary conditions must be set in order to obtain a unique solution. As (25) is an Euler equation in the whole space, if we look for almost-periodic solutions, it seems that no condition at infinity is needed. Also, a natural choice of initial conditions seems to be

$$\tilde{w}(y, 0) = w^0(y), \quad (27)$$

where we have omitted dependency upon large scale variables. However, any solution \tilde{w} of Euler equations (25) together with this initial condition presents some invariances which may be inconsistent with the physics of the problem. Concretely, we shall prove that the following statistics of \tilde{w} are τ -independent :

- Mean:

$$\bar{m} = \langle \tilde{w} \rangle = G^t \langle w \rangle; \quad (28)$$

- Mean Kinetic Energy:

$$q = \frac{1}{2} \langle \tilde{w} \cdot C^{-1} \tilde{w} \rangle = \frac{1}{2} \langle |w|^2 \rangle; \quad (29)$$

- Mean Helicity:

$$h = \frac{1}{2} \langle \tilde{w} \cdot C^{-1} \tilde{r} \rangle = \frac{1}{2} \langle w \cdot r \rangle, \text{ with } r = (G \nabla_y) \times w, \quad \tilde{r} = \nabla_y \times (C^{-1} \tilde{w}); \quad (30)$$

As the initial condition (27) does not depend upon the large scale time t , then w has constant (in t) mean kinetic energy and mean helicity. However, it is well known that in practice all statistics of the turbulent perturbation vary in time due to nonlinear effects and viscous dissipation. For this reason, it seems more convenient to consider the three statistics above as parameters determining the main fluctuation w , and try to obtain a solution of Euler equations (25) for each given value of these parameters. Our purpose in this section is to obtain on mathematical grounds the dependence of the fluctuation

w upon the parameters \tilde{m} , q and h ; by setting appropriate initial conditions for Euler equations (25).

Concretely, we shall set the following “universal” Euler problem for the pair (\tilde{w}^*, π^*) :

$$\left. \begin{aligned} \tilde{w}_{,\tau}^* + (\tilde{w}^* \cdot \nabla_y) \tilde{w}^* + C \nabla_y \pi^* &= 0, & \nabla_y \cdot \tilde{w}^* &= 0 & \text{in } \mathbb{R}^3 \times \mathbb{R} \\ \tilde{w}^*(y, 0) = \tilde{w}_0^*(y) = \frac{1}{\sqrt{q_0}} w^0\left(\frac{q_0}{h_0} y\right), & & & & \text{in } \mathbb{R}^3 \\ \tilde{w}^*, \pi^* & \text{almost-periodic in } (y, \tau), \end{aligned} \right\} \quad (31)$$

where q_0 and h_0 are the mean kinetic energy and mean helicity of the initial perturbation w_0 , respectively; assumed to be nonzero. Then we shall prove that, given the set of parameters $\tilde{m} \in \mathbb{R}^3$, $q \geq 0$, $h \in \mathbb{R}$, then the pair (\tilde{w}, π) defined by

$$\left. \begin{aligned} \tilde{w}(y, \tau) &= \sqrt{\tilde{q}} \tilde{w}^*\left(\frac{h}{\tilde{q}}(y - \tilde{m}\tau), \frac{q_0}{\sqrt{\tilde{q}}} \tau\right) + \tilde{m}; \\ \pi(y, \tau) &= \pi^*\left(\frac{h}{\tilde{q}}(y - \tilde{m}\tau), \frac{q_0}{\sqrt{\tilde{q}}} \tau\right); \\ \text{with } \tilde{q} &= q - \frac{1}{2} \tilde{m} \cdot C^{-1} \tilde{m}, \end{aligned} \right\} \quad (32)$$

is a solution of Euler equations (25) whose mean, mean kinetic energy and mean helicity are \tilde{m} , q and h , respectively.

Although it is possible to precise smoothness conditions on \tilde{w} and π under which our analysis holds, we shall always say that \tilde{w} ; π are “smooth enough”. This is so because we have no proof of convergence of our asymptotics expansions, so that we do not know what the exact regularity of \tilde{w} , π in particular should be.

Let us begin by proving the τ -invariance of the statistics of \tilde{w} (28), (29) and (30)

Proposition 1 *Assume $\det(G) = 1$ and assume Euler equations (25) admit a smooth solution (\tilde{w}, π) . Then the following equations hold :*

$$\tilde{w}_{,\tau} + \nabla_y \cdot [\tilde{w} \otimes \tilde{w} + C\pi] = 0, \quad \text{in } \mathbb{R}^3 \times \mathbb{R}; \quad (33)$$

$$\left(\frac{1}{2} \tilde{w} \cdot C^{-1} \tilde{w}\right)_{,\tau} + \nabla_y \cdot [\tilde{w} \left(\frac{1}{2} \tilde{w} \cdot C^{-1} \tilde{w} + \pi\right)] = 0, \quad \text{in } \mathbb{R}^3 \times \mathbb{R}; \quad (34)$$

$$\left(\tilde{w} C^{-1} \tilde{r}\right)_{,\tau} + \nabla_y \cdot [\tilde{w} (\tilde{w} \cdot C^{-1} \tilde{r}) + \tilde{r} (\pi - \frac{1}{2} \tilde{w} \cdot C^{-1} \tilde{w})] = 0, \quad \text{in } \mathbb{R}^3 \times \mathbb{R}; \quad (35)$$

where \tilde{r} is defined in (30).

Proof:

Equations (33) can be obtained from the Euler equation (25) and taking into account that $\nabla_y \cdot \tilde{w} = 0$.

To deduce (34), we multiply (25) by $\tilde{w} \cdot C^{-1}$ and then (34) follows.

We prove now (35). To do so, let us follow Ortegón ([22]): If $\det(G) = 1$, then

$$G^T[(G \nabla_y) \times \tilde{w}] = \nabla_y \times (C^{-1} \tilde{w}).$$

By taking the curl of (25), this formula yields the following evolution equation for \tilde{r} :

$$\tilde{r}_{,\tau} + (\tilde{w} \cdot \nabla_{\mathbf{y}})\tilde{r} - (\tilde{r} \cdot \nabla_{\mathbf{y}})\tilde{w} = 0, \quad \text{in } \mathbb{R}^3 \times \mathbb{R}. \quad (36)$$

Now, multiplying (36) by $\tilde{w} \cdot C^{-1}$ and (25) by $\tilde{r} \cdot C^{-1}$ and summing up these expressions, we have

$$(\tilde{w}C^{-1}\tilde{r})_{,\tau} + \tilde{w} \cdot \nabla_{\mathbf{y}}(\tilde{w} \cdot C^{-1}\tilde{r}) + \tilde{r} \cdot \nabla_{\mathbf{y}}(\pi - \frac{1}{2}\tilde{w} \cdot C^{-1}\tilde{w}) = 0.$$

and then, having in mind the incompressibility of \tilde{w} and \tilde{r} we obtain (35). ■

Corollary 1 *Assume $\det(G) = 1$. Assume Euler equations (25) admit an almost-periodic and smooth enough solution (\tilde{w}, π) . Then:*

i) The statistics (28)-(29) are τ -invariant.

ii) If in addition the rotational \tilde{r} is almost-periodic, then the statistic (30) is τ -invariant.

Proof: To prove (28), let us integrate equation (33) on $B_R \times [0, \tau]$ for a fixed $\tau \in \mathbb{R}$. This yields

$$\begin{aligned} \frac{1}{|B_R|} \int_{B_R} \tilde{w}(\mathbf{y}, \tau) d\mathbf{y} &= \frac{1}{|B_R|} \int_{B_R} \tilde{w}(\mathbf{y}, 0) d\mathbf{y} + \\ &+ \int_0^\tau \frac{1}{|B_R|} \int_{\Gamma_R} \tilde{n}(\mathbf{y}) \cdot (\tilde{w}(\mathbf{y}, \sigma) \otimes \tilde{w}(\mathbf{y}, \sigma) + C\pi(\mathbf{y}, \sigma)) d\Gamma_R(\mathbf{y}) d\sigma \end{aligned}$$

where $|B_R|$ is the volume of the ball B_R , Γ_R is the boundary of B_R and \tilde{n} is the unitary outward normal vector to Γ_R . As \tilde{w} and π are bounded, the boundary term in the right hand side vanishes as $R \uparrow \infty$.

The τ -invariance of (29) and (30) is proved similarly. ■

Remarks:

1. The hypothesis above that $\det(G) = 1$ can be formally proved from (26). Indeed, the second equation in (26), when $k = 2$, implies (See Section 5):

$$\nabla \cdot \mathbf{u} = 0, \quad \text{in } \mathbb{R}^3 \times \mathbb{R}.$$

Under regularity hypotheses on \mathbf{u} , this, together with (14), implies that the Jacobian

$$J = \det(G) = \det(\nabla a)$$

verifies the equation

$$J_{,t} + \mathbf{u} \cdot \nabla J = 0, \quad \text{in } \mathbb{R}^3 \times \mathbb{R}; \quad J(\mathbf{x}, 0) = 1 \quad \text{in } \mathbb{R}^3.$$

Consequently, $\det(G) = 1$ in $\mathbb{R}^3 \times \mathbb{R}$. ■

Let us now turn our attention to the derivation of expressions (33), that will determine the main perturbation terms in the expansions (5).

Proposition 2 *Assume the pair (\tilde{w}^*, π^*) is any smooth solution of Euler equations (25). Then, each pair (\tilde{w}, π) of the five-parameters family given by*

$$\left. \begin{aligned} \tilde{w}(y, \tau) &= \rho \tilde{w}^*(\lambda(y - \tilde{\alpha}\tau), \rho\lambda\tau) + \tilde{\alpha} \\ \pi(y, \tau) &= \rho^2 \pi^*(\lambda(y - \tilde{\alpha}\tau), \rho\lambda\tau) \end{aligned} \right\} \quad \forall \tilde{\alpha} \in \mathbb{R}^3, \quad \forall \lambda, \rho \in \mathbb{R} \quad (37)$$

is also solution of (25).

Proof: From (37) the operator $E(\tilde{w}, \pi; C)$ can be written as function of (\tilde{w}^*, π^*) as

$$E(\tilde{w}, \pi; C)(y, \tau) = \left[\rho \mu \tilde{w}_{,\tau}^* + \lambda \rho^2 (\tilde{w}^* \cdot \nabla_y) \tilde{w}^* + \sigma \lambda C \nabla_y \pi^* \right] (\lambda(y - \tilde{\alpha}\tau), \mu\tau)$$

Putting $\rho \mu = \lambda \rho^2 = \sigma \lambda$ and taking into account that (\tilde{w}^*, π^*) satisfies (25), we obtain $E(\tilde{w}, \pi; C) = 0$.

The incompressibility condition for \tilde{w} follows directly from that of \tilde{w}^* . ■

Remarks:

1. This multiplicity of solutions is due to certain symmetries of Euler equations (25). The most well known one is the so-called Galilean invariance, given by (37) when $\rho = \lambda = 1$. There are also invariance under re-scaling and under homotecies, given by (37) when $\tilde{\alpha} = \tilde{0}$, $\rho = 1$ and $\tilde{\alpha} = \tilde{0}$, $\lambda = 1$, respectively. These are all symmetries of Euler equations known to the authors. ■

Note that there is just one choice of parameters ρ, λ and $\tilde{\alpha}$ in (32) that allows to match all τ -invariants of \tilde{w} :

Proposition 3 *Assume that $\det(G) = 1$ and that the initial mean kinetic energy and helicity:*

$$q_0 = q_0(x) = \frac{1}{2} \langle w^0 \cdot C^{-1} w^0 \rangle, \quad h_0 = h_0(x) = \frac{1}{2} \langle w^0 \cdot C^{-1} (\nabla_y \times (C^{-1} w^0)) \rangle,$$

are non zero.

Assume also that the pair (\tilde{w}^, π^*) is a smooth solution of the Universal Euler problem (31) and that the curl of \tilde{w}^* , $\tilde{r}^* = \nabla_y \times (C^{-1} \tilde{w}^*)$ is almost-periodic. Then, for each $\tilde{m} \in \mathbb{R}^3$, $q \geq 0$, $h \in \mathbb{R}$, the velocity \tilde{w} given by (37) with*

$$\rho = \sqrt{\tilde{q}}, \quad \lambda = \frac{h}{\tilde{q}}, \quad \tilde{\alpha} = \tilde{m}, \quad \text{with } \tilde{q} = q - \frac{1}{2} \tilde{m} \cdot C^{-1} \tilde{m},$$

verifies

$$\langle \tilde{w} \rangle = \tilde{m}, \quad \frac{1}{2} \langle \tilde{w} \cdot C^{-1} \tilde{w} \rangle = q, \quad \frac{1}{2} \langle \tilde{w} \cdot C^{-1} \tilde{r} \rangle = h. \quad (38)$$

Proof:

We notice that the initial condition \tilde{w}_0^* in (31) has zero mean (due to (12)) and unit mean kinetic energy and mean helicity. Moreover, as \tilde{w}^* , \tilde{r}^* are almost-periodic in y , functions \tilde{w} , $\tilde{w} \cdot C^{-1} \tilde{w}$ and $\tilde{w} \cdot C^{-1} \tilde{r}$ are also almost-periodic and then, the averages values $\langle \tilde{w} \rangle$, $\langle \tilde{w} \cdot C^{-1} \tilde{w} \rangle$ and $\langle \tilde{w} \cdot C^{-1} \tilde{r} \rangle$ are well defined. To have (38), first we prove from (37) that

$$\begin{aligned} (a) \quad & \langle \tilde{w} \rangle (\tau) = \rho \langle \tilde{w}^* \rangle (\mu\tau) + \tilde{\alpha} \\ (b) \quad & \frac{1}{2} \langle \tilde{w} \cdot C^{-1} \tilde{w} \rangle (\tau) = \rho \left[\frac{1}{2} \rho \langle \tilde{w}^* \cdot C^{-1} \tilde{w}^* \rangle + \tilde{\alpha} \cdot C^{-1} \langle \tilde{w}^* \rangle \right] (\mu\tau) + \\ & \quad + \frac{1}{2} \tilde{\alpha} \cdot C^{-1} \tilde{\alpha} \\ (c) \quad & \frac{1}{2} \langle \tilde{w} \cdot C^{-1} \tilde{r} \rangle (\tau) = \frac{1}{2} \lambda \rho^2 \langle \tilde{w}^* \cdot C^{-1} \tilde{r}^* \rangle (\mu\tau) \tilde{r}(y, \tau) \end{aligned}$$

previously, we have proved that $\tilde{r}(y, \tau) = [\nabla_y \times C^{-1} \tilde{w}](y, \tau) = \rho \lambda \tilde{r}^*(\lambda(y - \tilde{\alpha}\tau), \mu\tau)$

The proof is similar in the three cases; for example,

$$\begin{aligned} \langle \tilde{w} \rangle (\tau) &= \lim_{R \rightarrow \infty} \frac{1}{|B_R|} \int_{B_R} \tilde{w}(y, \tau) dy = \\ &= \rho \lim_{R \rightarrow \infty} \frac{1}{|B_R|} \int_{B_R} \tilde{w}^*(\lambda(y - \tilde{\alpha}\tau), \mu\tau) dy + \tilde{\alpha} \end{aligned}$$

considering the changement of variables $z = \lambda y$ into the integral expression and in $|B_R|$, we have

$$\langle \tilde{w} \rangle (\tau) = \rho \lim_{R \rightarrow \infty} \frac{|\lambda|^{-n} \int_{B_{|\lambda|R}} \tilde{w}^*(z - \lambda \tilde{\alpha}\tau, \mu\tau) dz}{|\lambda|^{-n} \int_{B_{|\lambda|R}} dz} + \tilde{\alpha} = \rho \langle \tilde{w}^* \rangle (\mu\tau) + \tilde{\alpha}$$

Finally, putting $\rho = \sqrt{\tilde{q}}$, $\lambda = \frac{h}{\tilde{q}}$, $\tilde{\alpha} = \tilde{m}$, with $\tilde{q} = q - \frac{1}{2} \tilde{m} \cdot C^{-1} \tilde{m}$, we readily deduce (38). ■

Remarks:

1. The velocity field \tilde{w} given by Proposition 3 is a solution of the following problem:

$$\left. \begin{aligned} & \tilde{w}_{,\tau} + (\tilde{w} \cdot \nabla_y) \tilde{w} + C \nabla_y \pi = 0, \quad \nabla_y \cdot \tilde{w} = 0 \quad \text{in } \mathbb{R}^3 \times \mathbb{R}; \\ & \tilde{w}(y, 0) = \tilde{w}_0(y) \quad \text{in } \mathbb{R}^3; \\ & \tilde{w}, \pi \quad \text{almost-periodic in } (y - \tau) \\ & \text{where} \\ & \tilde{w}_0(y) = \sqrt{\frac{\tilde{q}}{q_0}} w^0\left(\frac{h}{h_0} \frac{q_0}{\tilde{q}} y\right) + \tilde{m}. \end{aligned} \right\} \quad (39)$$

Thus, \tilde{w}_0 appears as an appropriate initial condition for Euler equations (25), because it gives to the fluctuation \tilde{w} the degrees of freedom that are naturally associated to the structure of Euler equations. ■

In what follows, our analysis shall need the working hypothesis that this problem admits a unique almost-periodic solution, which depends smoothly upon (y, τ) and the parameter matrix C . This appears as an hypothesis very difficult to prove, as there are no results about existence of smooth global solutions of Euler equations in three space dimensions.

4 Determination of higher order terms

Let us now turn our attention to the determination of higher order terms in the asymptotic expansions (13). As the initial conditions for Navier-Stokes (10) do not contain terms in ϵ of order higher than $1/3$, an appropriate initial condition for the linear Euler-like equation (26) is

$$\tilde{u}^{(k)} = 0 \quad (40)$$

This initial condition avoids a given solution $(\tilde{u}^{(k)}, p^{(k)})$ of equation (26) to have a family of associated solutions similar to that given in Proposition 2 for Euler equations (25). Indeed, if (\tilde{u}_p, q_p) is a particular solution of (26),(40), then the general solution will be of the form

$$\tilde{u}^{(k)} = \tilde{u}_p + \tilde{u}_h; \quad p^{(k)} = q_p + q_h,$$

where (\tilde{u}_h, q_h) is the general solution of the homogeneous problem:

$$\left. \begin{aligned} L(\tilde{u}_h, q_h; \tilde{w}, C) = 0, \quad \nabla_y \cdot \tilde{u}_h = 0 & \quad \text{in } \mathbb{R}^3 \times \mathbb{R}; \\ \tilde{u}_h(x, 0) = 0 & \quad \text{in } \mathbb{R}^3. \end{aligned} \right\} \quad (41)$$

This equation does not possess as many symmetries as Euler equations (25). Indeed, the only solutions of (41) similar to (37) are given by

$$\left. \begin{aligned} \tilde{u}_h(y, \tau) &= \rho \tilde{u}_h^*(y - \tilde{\alpha}\tau, \lambda\tau); \\ \tilde{w}(y, \tau) &= \lambda \tilde{w}^*(y - \tilde{\alpha}\tau, \lambda\tau) + \tilde{\alpha}; \\ q_h(y, \tau) &= \rho \lambda q_h^*(y - \tilde{\alpha}\tau, \lambda\tau) \end{aligned} \right\} \quad \forall \tilde{\alpha} \in \mathbb{R}^3, \quad \forall \rho, \lambda \in \mathbb{R}; \quad (42)$$

where (\tilde{u}_h^*, q_h^*) is solution of (41) and \tilde{w}^* is a solution of (25). It is now clear that the only solution among those given in (42) that matches the initial conditions of (41) is $\tilde{u}_h \equiv 0$.

On another hand, there is still the possibility that system (26),(40) does not have any solutions at all. Indeed, to each conservation law of those given by (33), (34) and (35) for Euler equations (25), there corresponds a conservation law for the linear Euler equations (26), that force $\tilde{f}^{(k)}, g^{(k)}$ to verify certain compatibility conditions. This is stated as follows:

Proposition 4 *Let us assume that Euler equations (25) admit a smooth solution (\tilde{w}, π) , and that linearized Euler equations (26) admit too a smooth solution $(\tilde{u}^{(k)}, p^{(k)})$. Then the*

following equations hold:

$$\tilde{u}_{,\tau}^{(k)} + \nabla_{\mathbf{y}} \cdot [\tilde{w} \otimes \tilde{u}^{(k)} + \tilde{u}^{(k)} \otimes \tilde{w} + Cp^{(k)}] = \tilde{f}^{(k)} + \tilde{w}g^{(k)}, \quad \text{in } \mathbb{R}^3 \times \mathbb{R}; \quad (43)$$

$$\begin{aligned} & (\tilde{w} \cdot C^{-1} \tilde{u}^{(k)})_{,\tau} + \nabla_{\mathbf{y}} \cdot [\tilde{w}(\tilde{w} \cdot C^{-1} \tilde{u}^{(k)} + p^{(k)}) + \tilde{u}^{(k)}(\frac{1}{2} \tilde{w} \cdot C^{-1} \tilde{w} + \pi)] = \\ & = \tilde{w} \cdot C^{-1} \tilde{f}^{(k)} + (\frac{1}{2} \tilde{w} \cdot C^{-1} \tilde{w} + \pi)g^{(k)}, \end{aligned} \quad \text{in } \mathbb{R}^3 \times \mathbb{R}; \quad (44)$$

$$\begin{aligned} & (\tilde{w} \cdot C^{-1} \tilde{s}^{(k)} + \tilde{u}^{(k)} \cdot C^{-1} \tilde{r})_{,\tau} + \nabla_{\mathbf{y}} \cdot [\tilde{w}(\tilde{w} \cdot C^{-1} \tilde{s}^{(k)} + \tilde{u}^{(k)} \cdot C^{-1} \tilde{r}) + \tilde{s}^{(k)}(\pi - \frac{1}{2} \tilde{w} \cdot C^{-1} \tilde{w})] + \\ & + \nabla_{\mathbf{y}} \cdot [\tilde{r}(p^{(k)} - \tilde{w} \cdot C^{-1} \tilde{u}^{(k)}) + \tilde{u}^{(k)}(\tilde{w} \cdot C^{-1} \tilde{r})] = \tilde{w} \cdot C^{-1} \tilde{F}^{(k)} + \tilde{r} \cdot C^{-1} \tilde{f}^{(k)}, \end{aligned} \quad \text{in } \mathbb{R}^3 \times \mathbb{R}, \quad (45)$$

where $\tilde{r} = \nabla_{\mathbf{y}} \times (C^{-1} \tilde{w})$, $\tilde{s}^{(k)} = \nabla_{\mathbf{y}} \times (C^{-1} \tilde{u}^{(k)})$ and $\tilde{F}^{(k)} = \nabla_{\mathbf{y}} \times (C^{-1} \tilde{f}^{(k)})$.

Proof

Equations (43) is obtained directly from the linearised Euler equation (26) for $\tilde{u}^{(k)}$ and using the fact that $\nabla_{\mathbf{y}} \cdot \tilde{u}^{(k)} = g^{(k)}$.

To get (44), we multiply (25) by $\tilde{u}^{(k)} \cdot C^{-1}$ and (26) by $\tilde{w} \cdot C^{-1}$. Now, summing up these expressions, we obtain

$$(\tilde{w} \cdot C^{-1} \tilde{u}^{(k)})_{,\tau} + \tilde{w} \cdot \nabla_{\mathbf{y}} (\tilde{w} \cdot C^{-1} \tilde{u}^{(k)} + p^{(k)}) + \tilde{u}^{(k)} \cdot \nabla_{\mathbf{y}} (\frac{1}{2} \tilde{w} \cdot C^{-1} \tilde{w} + \pi) = \tilde{w} \cdot C^{-1} \tilde{f}^{(k)}$$

and (44) is readily derived having in mind that $\nabla_{\mathbf{y}} \cdot \tilde{u}^{(k)} = g^{(k)}$ and $\nabla_{\mathbf{y}} \cdot \tilde{w} = 0$. Also, taking the curl of (26) gives a transport equation for $\tilde{s}^{(k)}$:

$$\tilde{s}_{,\tau}^{(k)} + (\tilde{w} \cdot \nabla_{\mathbf{y}}) \tilde{s}^{(k)} + (\tilde{u}^{(k)} \cdot \nabla_{\mathbf{y}}) \tilde{r} - (\tilde{s}^{(k)} \cdot \nabla_{\mathbf{y}}) \tilde{w} - (\tilde{r} \cdot \nabla_{\mathbf{y}}) \tilde{u}^{(k)} = \tilde{F}^{(k)} - \tilde{r}g^{(k)}$$

Combining this equations with (25), (26) and (36), a similar derivation can be applied now to obtain (45) (cf. [13]). ■

Proposition 5 *i) Assume that \tilde{w} , π , $\tilde{u}^{(k)}$ and $p^{(k)}$ are almost-periodic and smooth enough. Then the following compatibility conditions hold:*

$$\ll \tilde{f}^{(k)} + \tilde{w}g^{(k)} \gg = 0, \quad (46)$$

$$\ll \tilde{w} \cdot C^{-1} \tilde{f}^{(k)} + (\frac{1}{2}(\tilde{w} \cdot C^{-1} \tilde{w}) + \pi)g^{(k)} \gg = 0, \quad (47)$$

$$\langle g^{(k)}(\cdot, \tau) \rangle = 0, \quad \forall \tau \in \mathbb{R} \quad (48)$$

ii) Assume in addition that the curls \tilde{r} and $\tilde{s}^{(k)}$ are almost-periodic. Then, the following compatibility condition also holds:

$$\ll \tilde{r} \cdot C^{-1} \tilde{f}^{(k)} \gg = 0. \quad (49)$$

Proof (Sketch):

To prove (46), for instance, let us average equation (43) in $B_R \times [-\tau, \tau]$. This yields:

$$\begin{aligned} & \frac{1}{2\tau|B_R|} \left[\int_{B_R} (\tilde{u}^{(k)}(y, \tau) dy - \tilde{u}^{(k)}(y, -\tau)) dy + \right. \\ & \left. + \int_{-\tau}^{\tau} \int_{\Gamma_R} \tilde{n}(y, \sigma) \cdot (\tilde{w} \otimes \tilde{u}^{(k)} + \tilde{u}^{(k)} \otimes \tilde{w} + Cp^{(k)})(y, \sigma) d\Gamma_R(y) d\sigma \right] = \\ & = \frac{1}{2\tau|B_R|} \int_{-\tau}^{\tau} \int_{B_R} (\tilde{f}^{(k)} + \tilde{w}g^{(k)})(y, \sigma) dy d\sigma \end{aligned}$$

As \tilde{w} , $\tilde{u}^{(k)}$ and $p^{(k)}$ are bounded, the left hand side vanishes as R and τ tend to infinity. Thus, (46) follows. The proof of (47) and (49) are similar.

Also, averaging the last equation in (26) on B_R yields

$$\frac{1}{|B_R|} \int_{\Gamma_R} (\tilde{n} \cdot \tilde{u}^{(k)})(y, \tau) d\Gamma_R(y) = \frac{1}{|B_R|} \int_{B_R} g^{(k)}(y, \tau) dy$$

As $\tilde{u}^{(k)}$ is bounded, the left hand side vanishes as $R \uparrow \infty$. Thus, (48) follows. ■

Remarks :

1. Note that these compatibility conditions are formally the same as those obtained in the original model described in [19], with a somewhat different microstructure problem. This is essentially due to the homogeneous character of the average operators considered in both cases. ■

In what follow we shall admit as working hypothesis that linear Euler equations (26) with initial conditions (40) admit a unique smooth almost-periodic solution $(\tilde{u}^{(k)}, p^{(k)})$ as soon as compatibility conditions (46)-(49) are fulfilled. Again we have to point out that we have no theoretical support for this hypothesis, but we need it to continue our analysis.

5 Averaged equations

In this Section we shall obtain the averaged equations of our model. This will yield the effective equations of the model, but also equations for the values of the parameters \tilde{m} , q and h needed to determine the main fluctuation terms (\tilde{w}, π) by (32). In particular, we shall prove that \tilde{m} is always zero. Moreover, we shall obtain explicitly the dependence of the closure terms of our model upon the parameters q and h .

Averaged equations are obtained in a natural way by implementing the compatibility conditions (46)-(49) for $k = 1, 2, \dots$. In the case $k = 1$ we obtain Euler equations for the pair (u, p) :

$$u_{,t} + (u \cdot \nabla)u + \nabla p = 0, \quad \nabla \cdot u = 0 \quad \text{in } \mathbb{R}^3 \times \mathbb{R}. \quad (50)$$

When $k = 2$, transport equations for the invariants of w are obtained:

1) **Mean** $m = \langle w \rangle$:

$$m_{,t} + (m \cdot \nabla)u + (u \cdot \nabla)m + \nabla \bar{p}^{(0)} = 0; \quad \nabla \cdot m = 0 \quad \text{in } \mathbb{R}^3 \times \mathbb{R}, \quad (51)$$

with $\bar{p}^{(0)} = \langle\langle p^{(0)} \rangle\rangle$.

2) **Mean Kinetic Energy** q :

$$q_{,t} + (u \cdot \nabla)q + \mathbf{R} : \nabla u + \mu \psi_q = 0, \quad \text{in } \mathbb{R}^3 \times \mathbb{R}, \quad (52)$$

where the tensor \mathbf{R} and the scalar function ψ_q are closure terms, defined by

$$\mathbf{R} = \langle\langle w \otimes w \rangle\rangle, \quad \psi_q = \langle\langle \tilde{r} \cdot C^{-1} \tilde{r} \rangle\rangle. \quad (53)$$

3) **Mean Helicity** h :

$$h_{,t} + (u \cdot \nabla)h + \mathbf{S} : \nabla u + \mu \psi_h = 0, \quad \text{in } \mathbb{R}^3 \times \mathbb{R}, \quad (54)$$

where the closure terms \mathbf{S} and ψ_h are defined by

$$\mathbf{S} = \langle\langle w \otimes r \rangle\rangle, \quad \psi_h = \langle\langle \tilde{r} \cdot C^{-1} (\nabla_v \times (C^{-1} \tilde{r})) \rangle\rangle. \quad (55)$$

When $k = 3$, a linear Reynolds equation for the mean velocity field

$$\bar{u}^{(1)} = \langle\langle u^{(1)} \rangle\rangle$$

appears:

$$\bar{u}_{,t}^{(1)} + (u \cdot \nabla)\bar{u}^{(1)} + (\bar{u}^{(1)} \cdot \nabla)u + \nabla \bar{p}^{(1)} + \nabla \cdot \mathbf{R} = 0, \quad \nabla \cdot \bar{u}^{(1)} = 0, \quad \text{in } \mathbb{R}^3 \times \mathbb{R} \quad (56)$$

with $\bar{p}^{(1)} = \langle\langle p^{(1)} \rangle\rangle$.

For the sake of simplicity, we shall not be interested in the remaining equations. In fact, the main features of the interactions between large and small scales are present in the equations above.

5.1 Obtention of averaged equations

Initial and conditions at infinity must be added to these equations in order to set well-posed problems. Although it is not clear how to set such conditions, we shall always look for bounded solutions. Also, initial conditions are derived in a natural way from (10). In particular, the initial condition for (51) is

$$m(x, 0) = 0$$

Consequently, if system (51) with this initial condition has a unique bounded solution, this must be given by

$$m \equiv 0, \quad \bar{p}^{(0)} \equiv \text{constant}.$$

The second equation above, together with (24), determines $p^{(0)}$ up to an arbitrary function of τ , that we may assume to be constant.

Remarks:

1. Equations (52) and (54) contain production terms with viscous dissipation effects. In particular, $\mu\psi_q$ is the rate of viscous dissipation of "turbulent" kinetic energy. Note that $\psi_q > 0$ as soon as the initial fluctuating velocity w^0 is nonzero.
2. Under our hypotheses of existence of a unique almost-periodic solution of the microstructure problem (39), all closure terms appearing in the averaged equations depend only on the parameters G , q and h . Equations (51), (52) and (54) provide the values of the parameters that determine the fluctuation w given by (32) and then, the closure terms.
3. Note also that an important consequence of almost-periodicity is that all closure terms are well defined. By "well defined" we mean that the limit that defines, for instance, \mathbf{R} .

$$\mathbf{R} = \lim_{R \rightarrow \infty, T \rightarrow \infty} \frac{1}{2T |B_R|} \int_{-T}^T \int_{B_R} w(y, \tau) \otimes w(y, \tau) dy d\tau$$

exists and is finite.

4. It is possible to find an equation for $\bar{u}^\epsilon = u + \epsilon^{1/3}w + \epsilon^{2/3}u^{(1)}$ by combining (50), (51) and (56). It is found

$$\bar{u}_{,t}^\epsilon + (\bar{u}^\epsilon \cdot \nabla)\bar{u}^\epsilon + \nabla \bar{p}^\epsilon + \epsilon^{2/3} \nabla \cdot \mathbf{R} = 0, \quad \nabla \cdot \bar{u}^\epsilon = 0, \quad (57)$$

where \mathbf{R} is computed from (53), (51), (52) and (54). This equation represents, in condensed form, the effects of the perturbation w on the mean velocity field, up to order ϵ . ■

Now, it is possible to give the dependence of closure terms on q and h , as a consequence of the symmetries of the microstructure problem (39). Indeed, let $\tilde{w}^* = \tilde{w}^*(C)$ be the canonical fluctuation given by (31). Then, (32) gives the solution of (39) as a function of \tilde{w}^* , q and h . A careful calculation of closure terms leads to (cf. [13]):

$$\left. \begin{aligned} \mathbf{R}(q, h; G) &= q G^{-T} \tilde{\mathbf{R}}^*(C) G^{-1}; & \psi_q(q, h; G) &= \frac{h^2}{q} \psi_q^*(C); \\ \mathbf{S}(q, h; G) &= h G^{-T} \tilde{\mathbf{S}}^*(C) G^{-1}; & \psi_h(q, h; G) &= \frac{h^3}{q^2} \psi_h^*(C); \end{aligned} \right\} \quad (58)$$

where

$$\left. \begin{aligned} \tilde{\mathbf{R}}^*(C) &= \ll \tilde{w}^*(C) \otimes \tilde{w}^*(C) \gg; & \psi_q^*(C) &= \ll \tilde{r}^*(C) \cdot C^{-1} \tilde{r}^*(C) \gg; \\ \tilde{\mathbf{S}}^*(C) &= \ll \tilde{r}^*(C) \otimes \tilde{w}^*(C) \gg; & \psi_h^*(C) &= \ll \tilde{r}^*(C) \cdot C^{-1} (\nabla_{\mathbf{y}} \times C^{-1} \tilde{r}^*(C)) \gg. \end{aligned} \right\} \quad (59)$$

Let us see how we can get, for example, the expression for $\psi_q(q, h; G)$. To do so, we express

at first \tilde{r} in function of \tilde{r}^* : $\tilde{r}(y, \tau) = \frac{h}{\sqrt{q}} \tilde{r}^* \left(\frac{h}{q} y, \frac{h}{\sqrt{q}} \tau \right)$. Thus,

$$\begin{aligned} \psi_q(q, h; G) &= \lim_{(R, \tau) \rightarrow \infty} \frac{1}{2\tau |B_R|} \int_{-\tau}^{\tau} \int_{B_R} (\tilde{r} \cdot C^{-1} \tilde{r})(y, \sigma) dy d\sigma = \\ &= \frac{h^2}{q} \lim_{(R, \tau) \rightarrow \infty} \frac{1}{2\tau |B_R|} \int_{-\tau}^{\tau} \int_{B_R} (\tilde{r}^* \cdot C^{-1} \tilde{r}^*) \left(\frac{h}{q} y, \frac{h}{\sqrt{q}} \sigma \right) dy d\sigma. \end{aligned}$$

Now, we consider that $|B_R| = \int_{B_R} dy$, and we make the changements of variables $z = \frac{h}{q} y$ and $\delta = \frac{h}{\sqrt{q}} \sigma$. This yields, after some algebra,

$$\psi_q(q, h; G) = \frac{h^2}{q} \lim_{(R, \tau) \rightarrow \infty} \frac{\int_{-\frac{h}{\sqrt{q}}\tau}^{\frac{h}{\sqrt{q}}\tau} \int_{B_{|\frac{h}{q}|R}} (\tilde{r}^* \cdot C^{-1} \tilde{r}^*)(z, \delta) dz d\delta}{2 \left(\frac{h}{\sqrt{q}} \tau \right) \int_{B_{|\frac{h}{q}|R}} dz} = \frac{h^2}{q} \ll \tilde{r}^*(C) \cdot C^{-1} \tilde{r}^*(C) \gg.$$

■

Now, our system of averaged equations, including the Lagrangian coordinates, is the following:

$$\left. \begin{aligned} u_{,t} + (u \cdot \nabla)u + \nabla p &= 0, & \nabla \cdot u &= 0 & \text{in } \mathbb{R}^3 \times \mathbb{R}, \\ u(x, 0) &= u_0(x) & & & \text{in } \mathbb{R}^3; \\ a_{,t} + (u \cdot \nabla)a &= 0, & & & \text{in } \mathbb{R}^3 \times \mathbb{R}, \\ a(x, 0) &= x & & & \text{in } \mathbb{R}^3; \\ q_{,t} + (u \cdot \nabla)q + q \left[(G^{-T} \tilde{\mathbf{R}}^*(C) G^{-1}) : \nabla u + \mu \left(\frac{h}{q} \right)^2 \psi_q^*(C) \right] &= 0 & & & \text{in } \mathbb{R}^3 \times \mathbb{R}, \\ q(x, 0) &= q_0(x) = \frac{1}{2} \langle |w^0(\cdot, x)|^2 \rangle & & & \text{in } \mathbb{R}^3; \\ h_{,t} + (u \cdot \nabla)h + h \left[(G^{-T} \tilde{\mathbf{S}}^*(C) G^{-1}) : \nabla u + \mu \left(\frac{h}{q} \right)^2 \psi_h^*(C) \right] &= 0 & & & \text{in } \mathbb{R}^3 \times \mathbb{R}, \\ h(x, 0) &= h_0(x) = \frac{1}{2} \langle w^0(\cdot, x) \cdot (\nabla_{\mathbf{y}} \times w^0(\cdot, x)) \rangle & & & \text{in } \mathbb{R}^3; \\ \bar{u}_{,t}^{(1)} + (u \cdot \nabla) \bar{u}^{(1)} + (\bar{u}^{(1)} \cdot \nabla)u + \nabla \bar{p}^{(1)} + \nabla \cdot (q G^{-T} \tilde{\mathbf{R}}^*(C) G^{-1}) &= 0 & & & \text{in } \mathbb{R}^3 \times \mathbb{R}, \\ \nabla \cdot \bar{u}^{(1)} &= 0 & & & \text{in } \mathbb{R}^3 \times \mathbb{R}, \\ u^{(1)}(x, 0) &= 0 & & & \text{in } \mathbb{R}^3. \end{aligned} \right\} \quad (60)$$

Solving (60), we obtain an approximation to the average value of u^ϵ of (theoretical) order ϵ , given by $u + \epsilon^{2/3} \bar{u}^{(1)}$.

Remarks:

1. This system is formally the same as the one obtained in the original model (cf. [23]); although the definition of the average operator is somewhat different. This is a consequence of the homogeneity of the average operators considered in both models. Thus, in both models we obtain a formal mathematical modelling of locally homogeneous turbulence for flows with two well separated space scales.
2. Note that system (60) is formally closed, as all closure terms are (theoretically) computable functions of q , h and G . The only coupling in this system arises between the equations for q , h and (39) for the fluctuation w .
3. From a practical point of view, system (60) must be solved "in cascade": First obtain u , p , and then obtain the Lagrangian coordinates a . Next solve the coupled equations for q , h and (39) for the fluctuation w ; and finally, obtain $\bar{u}^{(1)}$.

However, solving an equation (39) for each $(x, t) \in \mathbb{R}^3 \times \mathbb{R}$ turns out to be an unfeasible task. As problem (39) depends only on the parameters C , q and h , it is much more practical to compute previously all closure terms as functions of these parameters. Note that closure terms are "universal", in the sense that they do not depend directly on the actual initial conditions for (60). ■

6 Connection with classical turbulence modelling

In this Section we shall analyze some analogies and differences of physical relevance between our model and “classical” two-equations models of turbulence. We shall show that our model can be considered as a two-equations model for locally homogeneous turbulence in Kolmogorov’s equilibrium range. In this context, we shall observe that our model predicts the existence of certain transient effects in the interaction large-small scales that are not taken into account by usual models of turbulence. From another hand, we shall observe that our model needs a further improvement to predict eddy diffusion effects. Moreover, we shall see that the role of the equation for the statistic h in our model, is to drive the effect of the viscosity from the small scales to the mean flow; in the sense that h acts on the mean flow only if the turbulent perturbation lies on the viscous subrange of the Kolmogorov’s equilibrium one.

Using the usual terminology in classical turbulence modelling, we can say that our model applies to “locally homogeneous turbulence” in Kolmogorov’s equilibrium range. Indeed, the “turbulence” is locally homogeneous because our average operator (15) is invariant under space-time translations, on the class of almost periodic functions. Note that we are not in general dealing with “locally isotropic turbulence” in the classical sense, although our average operator is itself isotropic in space. As we shall show in Section 7, the turbulent perturbation w will be isotropic only if the initial one w^0 is isotropic.

Also, we can show that the perturbation w lies on Kolmogorov’s equilibrium range by means of our asymptotic analysis. Let us recall that the characteristic velocity and length scales of our turbulent perturbation are $\epsilon^{1/3}$ and ϵ , respectively. Then, the associated Kolmogorov’s viscous scale is $\epsilon^{4/3}$. Thus, no equilibrium range may exist if the inverse Reynolds number in Navier-Stokes equations (9) is of order $\epsilon^{-4/3}$. An asymptotic analysis similar to that of Sections 1, 2 and 3 leads to the following equation for \tilde{w} (cf. [6]):

$$\left. \begin{aligned} \tilde{w}_{,\tau} + (\tilde{w} \cdot \nabla_y) \tilde{w} + C \nabla_y \pi - \mu \nabla_y \cdot (C \nabla_y \tilde{w}) &= 0, & \nabla_y \cdot \tilde{w} &= 0 & \text{in } \mathbb{R}^3 \times \mathbb{R} \\ \tilde{w}(y, 0) &= \tilde{w}_0(y) & & & \text{in } \mathbb{R}^3 \\ \tilde{w} &\text{ almost-periodic in } (y - \tau). \end{aligned} \right\}$$

Then, \tilde{w} must decay exponentially in time, so that all its statistics vanish. Consequently, viscous dissipation is shown to damp all turbulent effects in an infinitesimal time.

The higher level of viscosity for which our analysis shows the existence of an equilibrium range of eddies is just ϵ^2 , as considered in the initial problem (9). In this case, our analysis yields that the turbulent perturbation w depends only on the two statistics q and h (See (39)), in accordance with the first Kolmogorov’s hypothesis. A classical consequence of this hypothesis is that all statistics of the turbulent perturbation may be calculated by

means of dimensional analysis from just two dimensionally independent statistics (usually, the kinematic viscosity ν and the rate of decay of turbulent kinetic energy e). This is also the case in our model: The structures of \mathbf{R} , \mathbf{S} , ψ_q and ψ_h given in (60) are just the ones that could be constructed from q and h by means of dimensional analysis. However, in our case these structures have been calculated analytically starting from (39).

Now, model (61) appears as a two-equations model for locally homogeneous turbulence with two well-separated space scales. It resembles formally to classical models such as $k-\epsilon$ or $k-l$ models (cf. [17, 26, 27]), with the second statistic (ϵ or l) being replaced by the mean turbulent helicity h . Model (60) takes into account some of the main effects that govern the statistical behaviour of the turbulent perturbation, namely transport by the mean velocity field, production due to interaction with the mean flow and viscous dissipation. However, no turbulent diffusion is taken into account in it. Indeed, it was remarked in [19] that MPP models conserve the total kinetic energy. Then, the mathematical nature of tensor \mathbf{R} could be hyperbolic rather than elliptic. Some numerical simulations of the interactions between mean flow and nonhelical microstructures have shown that the role of tensor \mathbf{R} is to model some transient effects of the turbulence for flows in two scales that usual turbulence models are unable to reproduce. Concretely, in [7] an oscillatory behaviour of the interactions between large and small scales in three-dimensional homogeneous turbulence for Poiseuille flow was observed. In this paper we also present some numerical results that show that this oscillatory behaviour occurs also when the small structures are helical (i.e., $h \neq 0$) (cf. Section 9). Also, a comparison between a $k-\epsilon$ transient model and a MPP model including q and not h was made in [3] for two-dimensional flow past a cylinder. This experiment indicates that the production terms in the MPP model are relevant in regions where strong transient effects take place. While the $k-\epsilon$ model fails to simulate appropriately these effects, in most cases however it seems that viscous effects dominate transient effects. This seems to confirm the conjecture of [19] that tensor \mathbf{R} is of hyperbolic character.

Up to now, we have stated that model (60) does not contain eddy diffusion terms. However, eddy diffusion is found if we write the fourth order averaged equations. Concretely, the following equation for the mean velocity field is proposed in [6]:

$$\bar{u}_t^\epsilon + (\bar{u}^\epsilon \cdot \nabla) \bar{u}^\epsilon + \nabla \bar{p}^\epsilon + \epsilon^{2/3} \nabla \cdot \tilde{\mathbf{R}}^* = \nu_t \epsilon^{4/3} \nabla \cdot [\sqrt{q} (\nabla \bar{u}^\epsilon + (\nabla \bar{u}^\epsilon)^t)], \quad (61)$$

where $\bar{u}^\epsilon = u + \epsilon^{2/3} \bar{u}^{(1)} + \epsilon \bar{u}^{(2)} + \epsilon^{4/3} \bar{u}^{(3)}$ and ν_t is an eddy viscosity coefficient. Equation (61) is an extension of (57) that provides a (theoretically) more accurate approximation to the mean velocity field.

On the hand, the similarities of model (60) with classical models of turbulence is particularly made apparent when the initial mean velocity field u_0 is constant. In this case, model (60) reduces to a classical $k-\epsilon$ model for globally isotropic turbulence. Indeed,

now the mean velocity field \bar{u} is constant, and the equations for q and h can be combined to give an equation for the rate of viscous dissipation e of mean kinetic energy,

$$e = \mu \langle |\nabla_{\mathbf{y}} w|^2 \rangle = \mu \langle |\nabla_{\mathbf{y}} \times w|^2 \rangle = \mu \frac{h^2}{q} \psi_q^*, \text{ with } \psi_q^* = \psi_q^*(I).$$

This model is the following:

$$\left. \begin{aligned} q_{,t} + e &= 0, \\ e_{,t} + d \frac{e^2}{q} &= 0. \end{aligned} \right\} \quad (62)$$

where $d = 2 \frac{\psi_h^*}{\psi_q^*} - 1$. In the classical theory of isotropic turbulence, model (62) is also obtained solely by means of dimensional analysis, and it is assumed to model globally isotropic turbulence (cf. [27]). Also, the numerical constant d is obtained from experimental results and assumed to be universal in the sense that it is the same for similar experiments. Here, we obtain d analytically from the universal microstructure problem (31) with $C = I$. Note that this constant d may take different values for similar experiments, as it depends on the initial perturbation field w^0 . However, it is also universal in the sense that it depends only upon w^0 and not on the actual value of the viscosity coefficient μ . Model (62) can be integrated analytically to give, when $\psi_q^* \neq \psi_h^*$:

$$\left. \begin{aligned} q(t) &= q_0 \left(1 + \frac{t}{\tau}\right)^{-\gamma}, \quad e(t) = e_0 \left(1 + \frac{t}{\tau}\right)^{-(\gamma+1)}, \quad h(t) = h_0 \left(1 + \frac{t}{\tau}\right)^{-(\gamma+1/2)}, \\ \text{with } \gamma &= \frac{1}{d-1}, \quad e_0 = \mu \frac{h_0^2}{q_0} \psi_q^*, \quad \tau = \gamma \frac{q_0}{e_0}. \end{aligned} \right\}$$

In the classical theory of isotropic turbulence, it is possible to set the parameter γ in such a way that the values of q and e above correspond to a simple model of energy spectrum containing the Kolmogorov's law in $k^{-5/3}$ for the inertial range. For instance, in [27], this model spectrum is

$$\left. \begin{aligned} E(k) &= A q^m && \text{if } k_0 \leq k \leq k_M \text{ with } m > 0, \\ E(k) &= B e^{2/3} k^{-5/3} && \text{if } k_M \leq k \leq k_D. \end{aligned} \right\}$$

Here, k_0 is the wavenumber corresponding to the largest structures in the flow, k_M is the wavenumber of the eddies carrying the maximum of energy and k_D is the wavenumber associated to viscous dissipation. Also, A and B are numerical constants. In [27] it is formally proved that it is possible to obtain an inertial range associated to the spectrum above if

$$\gamma = 2 - \frac{4}{m+3} > 0.$$

We have performed some preliminar numerical experiments to solve the equation for the canonical microstructure equation (31). We use Crank-Nicholsol scheme in time, with

a spectral Fourier discretization in space. This scheme conserves mean, kinetic energy and helicity of the initial condition. Using a $8 \times 8 \times 8$ mesh and taking for instance a Beltrami flow as initial condition \tilde{w}_0^* , we obtain $\gamma = 2.17$, which fits into this framework.

This seems to support the fact that our theory agrees in the case of constant mean flow with the classical theory of isotropic turbulence. However, we do not know whether it is possible to prove analytically the derivation of the spectrum above in the framework of our theory.

Let us remark also that model (60) suggests that two-equations models of turbulence including the statistic h (mean turbulent helicity), in addition to q (mean turbulent energy), may be more appropriate to simulate turbulence with two space scales than those including e (rate of viscous dissipation of mean kinetic energy) or some alternative statistic of the turbulent perturbation, instead of h . We have mainly two reasons to think so. Let us remark at first that when the Reynolds number in Navier-Stokes equations (9) is of order $\epsilon^{-7/3}$ or higher, the equation for h in (60) decouples from the remaining equations, and may be eliminated from the model. This fact may be interpreted in the framework of classical modelling of turbulence, in the sense that in this case the turbulent perturbation w is fully inside the inertial range. Thus, the statistical properties of the turbulent perturbation may be described by means of just one of its statistics (In the case, q). Note also that both statistics q and h appear in a natural way in our model, as a consequence of the existence of certain conservation laws verified by the turbulent perturbation. In opposition, the statistics that are commonly used when constructing two-equations models of turbulence are chosen following reasons of physical nature, which may be somehow heuristic. However, we do not know whether the two statistics q and h are in some sense particularly appropriate to simulate eddy viscosity effects.

Let us remark finally that the role of the helicity in our model is to drive the effect of the viscosity from the small scales to the mean flow, because it is active only if the perturbation w lies on the viscous subrange.

7 Local isotropy

In this section we analyze some properties of physical relevance of our model that occur when the initial perturbation is locally isotropic. We give a mathematical proof that in this case the canonic turbulent perturbation is locally statistically isotropic at any time. We also prove that in its turn this implies the frame invariance of model (60). Thus, frame invariance will appear as a natural consequence of the local isotropicity of the initial perturbation.

We shall begin by setting specific concepts of isotropy for vector functions, and also of

“statistical” isotropicity for the canonical fluctuation \tilde{w}^* :

Definition 1 : Let $v : \mathbb{R}^3 \rightarrow \mathbb{R}$ be a vector function. We shall say that v is isotropic if $v(Qy) = Qv(y)$, for all $y \in \mathbb{R}^3$, for all rotation matrix Q .

Definition 2 : Let $v(C; \cdot) : \mathbb{R}^3 \rightarrow \mathbb{R}^3$ be an almost-periodic vector function for each 3×3 matrix C . We shall say that v is statistically isotropic at matrix C if

$$\langle v_{i_1}(Q^T C Q; \cdot), \dots, v_{i_k}(Q^T C Q; \cdot) \rangle = Q_{j_1 i_1} \cdots Q_{j_k i_k} \langle v_{j_1}(C; \cdot), \dots, v_{j_k}(C; \cdot) \rangle,$$

for all integer $k \geq 1$, for all $i_1, \dots, i_k \in 1, 2, 3$ and for all rotation matrix Q .

Definition 3 : Let $\tilde{w}^*(C; y, \tau)$ the solution of the universal microstructure problem (31). We shall say that \tilde{w}^* is statistically isotropic if it is statistically isotropic at any 3×3 symmetric matrix C with determinant one.

Let us now analyze the dependence of the canonical fluctuation \tilde{w}^* upon the matrix C :

Proposition 6 : Assume the canonical microstructure problem (31) has a unique smooth solution $(\tilde{w}^*(C; y, \tau), \pi^*(C; y, \tau))$. Assume also the initial perturbation w^0 is isotropic. Then, for each rotation matrix Q we have

$$\left. \begin{aligned} \tilde{w}^*(Q^T C Q; y, \tau) &= Q^T \tilde{w}^*(C; Qy, \tau) \\ \pi^*(Q^T C Q; y, \tau) &= \pi^*(C; Qy, \tau) \end{aligned} \right\} \quad \forall y \in \mathbb{R}^3, \quad \forall \tau \in \mathbb{R}. \quad (63)$$

Proof:

Let us define the following transformations:

$$Y = Q^T y, \quad \tilde{W}^*(Y, \tau) = Q^T \tilde{w}^*(C; y, \tau); \quad \Pi^*(Y, \tau) = \pi^*(C; y, \tau).$$

Now, we can express all terms in (25) as

$$\tilde{W}_{,\tau}^*(Y, \tau) = Q^T \tilde{w}_{,\tau}^*(y, \tau), \quad ((\tilde{W}^* \cdot \nabla_Y) \tilde{W}^*)(Y, \tau) = Q^T ((\tilde{w}^* \cdot \nabla_y) \tilde{w}^*)(y, \tau),$$

$$(Q \nabla_Y \Pi^*)(Y, \tau) = (\nabla_y \pi^*)(y, \tau), \quad (\nabla_Y \cdot \tilde{W}^*)(Y, \tau) = (\nabla_y \cdot \tilde{w}^*)(y, \tau)$$

And so

$$\tilde{W}_{,\tau}^* + (\tilde{W}^* \cdot \nabla_Y) \tilde{W}^* + (Q^T C Q) \nabla_Y \Pi^* = 0, \quad \nabla_Y \cdot \tilde{W}^* = 0$$

and the initial condition is given by

$$\tilde{W}^*(Y, 0) = Q^T \tilde{w}^*(C; QY, 0) = Q^T \tilde{w}_0^*(QY)$$

Moreover, as (\tilde{w}^*, π^*) is almost-periodic in (y, τ) so it does (\tilde{W}^*, Π^*) , and then it verifies:

$$\left. \begin{aligned} \tilde{W}_{,\tau}^* + (\tilde{W}^* \cdot \nabla_Y) \tilde{W}^* + (Q^T C Q) \nabla_Y \Pi^* &= 0, \quad \nabla_Y \cdot \tilde{W}^* = 0 && \text{in } \mathbb{R}^3 \times \mathbb{R}, \\ \tilde{W}^*(Y, 0) &= Q^T \tilde{w}_0^*(QY) && \text{in } \mathbb{R}^3, \\ \tilde{W}^*, \Pi^* &\text{ almost-periodic in } (y - \tau). \end{aligned} \right\}$$

As w^0 is isotropic, then \tilde{w}_0^* is also isotropic (i.e. $\tilde{w}_0^*(Q^T y) = Q^T \tilde{w}_0^*(y) \forall y \in \mathbb{R}^3$, $\forall Q \in O_+^3$) and (\tilde{W}^*, Π^*) is a solution of (31) with matrix $Q^T C Q$ instead of C . Under our hypothesis of unicity of solutions of (31), this yields (63) ■

Corollary 2 : *Under the hypotheses of Proposition 6, the fluctuation \tilde{w}^* is statistically isotropic. In particular, the canonical closure terms verify*

$$\left. \begin{aligned} \tilde{\mathbf{R}}^*(Q^T C Q) &= Q^T \tilde{\mathbf{R}}^*(C) Q, \quad \psi_q^*(Q^T C Q) = \psi_q^*(C), \\ \tilde{\mathbf{S}}^*(Q^T C Q) &= Q^T \tilde{\mathbf{S}}^*(C) Q, \quad \psi_h^*(Q^T C Q) = \psi_h^*(C), \end{aligned} \right\} \quad (64)$$

for all rotation matrix Q , for all 3×3 symmetric matrix C with determinant one.

Proof: The statistical isotropicity of \tilde{w}^* is an immediate consequence of (63) and the invariance under rotations of the space average operator defined in (11). Also, (64) follows directly from (63) for the same reasons. ■

These structures can be used now to simplify notably the dependence of closure terms on the matrix C as follows:

Proposition 7 : *Let G be a 3×3 matrix with determinant one and $\bar{C} = GG^t$. Let us denote by $i_1 = \text{trace}(\bar{C})$ and $i_2 = \text{trace}(\text{Adj}(\bar{C}))$ the two nontrivial invariants of \bar{C} . Then, under the hypotheses of Proposition 6, the following statements hold:*

i) *There exist six functions $\alpha_0, \alpha_1, \alpha_2, \beta_0, \beta_1, \beta_2$, which depend only upon i_1 and i_2 , such that*

$$\left. \begin{aligned} \mathbf{R}(q, h; G) &= q[\alpha_0(i_1, i_2)I + \alpha_1(i_1, i_2)\bar{C} + \alpha_2(i_1, i_2)\bar{C}^2]; \\ \mathbf{S}(q, h; G) &= h[\beta_0(i_1, i_2)I + \beta_1(i_1, i_2)\bar{C} + \beta_2(i_1, i_2)\bar{C}^2]. \end{aligned} \right\}$$

ii) *There exist two functions $\tilde{\psi}_q, \tilde{\psi}_h$, which depend only upon i_1 and i_2 , such that*

$$\psi_q(q, h; G) = \frac{h^2}{q} \tilde{\psi}_q(i_1, i_2); \quad \psi_h(q, h; G) = \frac{h^3}{q^2} \tilde{\psi}_h(i_1, i_2).$$

Proof: i) Due to (64), tensor $\tilde{\mathbf{R}}^*$ verifies the hypotheses of Rivlin-Ericksen's theorem (cf. [9]). Then, there must exist three functions $\tilde{\alpha}_0, \tilde{\alpha}_1$ and $\tilde{\alpha}_2$ depending only upon the two nontrivial invariants \tilde{i}_1 and \tilde{i}_2 of C , such that

$$\tilde{\mathbf{R}}^*(C) = \tilde{\alpha}_0(\tilde{i}_1, \tilde{i}_2)I + \tilde{\alpha}_1(\tilde{i}_1, \tilde{i}_2)C + \tilde{\alpha}_2(\tilde{i}_1, \tilde{i}_2)C^2.$$

Let us recall now that matrix C verifies its characteristic equation (Cayley-Hamilton's Theorem):

$$C^3 - \text{trace}(C)C^2 + \text{trace}(\text{Adj}(C))C - \det(C)I = 0.$$

Moreover, $\text{trace}(C) = i_1$ and $\text{trace}(\text{Adj}(C)) = \text{trace}(C^{-1}) = \text{trace}(\bar{C}^{-1}) = i_2$. Then, the first conclusion of i) follows, with

$$\alpha_0 = \tilde{\alpha}_1 + i_2 \tilde{\alpha}_0; \quad \alpha_1 = \tilde{\alpha}_2 - i_1 \tilde{\alpha}_0; \quad \alpha_2 = \tilde{\alpha}_0$$

A similar deduction holds for tensor \tilde{S}^* .

ii) From (64) it follows that ψ_q^* and ψ_h^* must depend only upon the invariants of C . This is due to the fact that a symmetric matrix can be diagonalized by means of orthogonal matrices. Then, (58) yields the conclusion of ii). ■

Remarks:

1. Note that in practice, the structures given by Proposition 7 reduce to two the number of parameters of tabulation in the canonical microstructure problem (31). This tabulation has been implemented numerically by Ortegón, who with a definition of isotropy less restrictive than ours, computed periodic steady fluctuations \tilde{w}^* (cf. [23]).

■

Our main result in this Section is the following:

Proposition 8 : *Assume the canonic fluctuation \tilde{w}^* is locally statistically isotropic. Then model equations (60) are frame-invariant.*

Proof: (Sketch)

Let us consider a rotation matrix Q , and define the following transformed magnitudes:

$$X = Qx, \quad U(X, t) = Q u(x, t), \quad E(X, t) = q(x, t), \quad H(X, t) = h(x, t), \quad \text{for } x \in \mathbb{R}^3, \quad t \in [0, T].$$

Let $A(X, t)$ be the Lagrangian coordinates associated to the velocity field $U(X, t)$, i.e.

$$A_{,t} + (U \cdot \nabla_X) A = 0, \quad A(X, 0) = X$$

then

$$A(X, t) = Q a(x, t),$$

and consequently

$$(\nabla_x a)(x, t) = Q^T (\nabla_X A)(X, t) Q.$$

Furthermore,

$$u \nabla_x q(x, t) = U \nabla_X E(X, t).$$

With these transformations, the equation in (60) for q becomes

$$E_{,t} + (U \cdot \nabla_X) E + E \left[F^{-T} Q \tilde{\mathbf{R}}^* (Q^T B Q) Q^T F^{-1} : (\nabla_X U) + \mu \left(\frac{H}{E} \right)^2 \psi_q^* (Q^T B Q) \right] = 0, \quad (65)$$

where we have denoted

$$F = \nabla_X A, \quad B = F^T F.$$

To obtain (65), we have considered that

$$M_1 : M_2 M_3 M_4 = M_2^T M_1 M_4^T : M_3,$$

for all square matrices M_1, M_2, M_3, M_4 of any order.

Now, as the fluctuation \tilde{w}^* is statistically isotropic, then (64) holds, and equation (65) is transformed into

$$E_{,t} + (U \cdot \nabla_X) E + E \left[F^{-T} \tilde{\mathbf{R}}^*(B) F^{-1} : (\nabla_X U) + \mu \left(\frac{H}{E} \right)^2 \psi_q^*(B) \right] = 0.$$

Consequently, the equation in (60) for q is frame-invariant. An analogous deduction holds for the remaining equations in (60). ■

Corollary 3 : *If the initial perturbation w^0 is isotropic, then model equations are frame-invariant.* ■

Remarks:

1. Note that to prove that model equations (60) are frame-invariant we only need the identities (64) and not the stronger condition that the canonic fluctuation \tilde{w}^* is locally isotropic. In [23] Ortégón proves also that if model equations (60) are frame-invariant, then (64) holds. Thus, the frame invariance of our model is equivalent to the isotropy of all closure terms (i.e., conditions (64)).
2. Note that the conclusion of Corollary 3 could not be deduced in the precedings MPP models. Indeed, in these models the microstructure problem considered is

$$\left. \begin{aligned} \tilde{w}_{,\tau} + (\tilde{w} \cdot \nabla_y) \tilde{w} + C \nabla_y \pi &= 0, & \nabla_y \cdot \tilde{w} &= 0 & \text{in } \mathbb{R}^3 \times \mathbb{R}, \\ \tilde{w}(y, 0) &= w^0(y) & & & \text{in } \mathbb{R}^3, \\ \tilde{w}, \pi & & (y, \tau) & \text{periodic with period cell } [0, 2\pi]^3 \times [0, 2\pi], & \end{aligned} \right\}$$

where w^0 is supposed to be periodic with period cell $[0, 2\pi]^3$.

This problem is invariant only under rotations Q that leave unchanged the cube Y , because periodicity must be conserved. Consequently, (64) do not hold for all rotations.

3. Speziale sets in [29] some necessary conditions for a turbulence model to be frame-invariant, when the frame of reference is inertial and also when it is not inertial. Here we have proved only the frame invariance when the frame is non-inertial.
4. Although we are able to prove that if w^0 is isotropic, then our model is frame-invariant, we are not able to prove whether this still occurs or not when w^0 is not isotropic.

8 Numerical experiments

In this Section we shall test a version of our model that applies to helical turbulence, in the case of 3D Poiseuille flow. Our purpose is to perform a numerical solution of the model and also of Navier-Stokes equations separately, and then to compare suitably the results of both simulations.

8.1 Direct Numerical simulation with Navier-Stokes equations

We shall consider incompressible viscous flow in the domain

$$\Omega = \mathbb{R} \times \mathbb{R} \times]0, 2[.$$

Periodicity is asked in the x_1 and x_2 directions, and no-slip boundary conditions are imposed on the walls $x_3 = 0$ and $x_3 = 2$. If we denote by ν the inverse Reynolds number, then this flow satisfies the Navier-Stokes equations

$$U_{,t} + (U \cdot \nabla)U - \nu \Delta U = 0, \quad \nabla \cdot U = 0 \quad \text{in } \Omega \times \mathbb{R}^+, \quad (66)$$

together with the following boundary conditions:

$$U(x_1 + \frac{2\pi}{\alpha_1}j, x_2 + \frac{2\pi}{\alpha_2}k, x_3; t) = U(x_1, x_2, x_3; t), \quad \forall (x_1, x_2, x_3; t) \in \Omega \times \mathbb{R}^+ \quad (67)$$

for any integer numbers j, k ; and

$$U(x_1, x_2, x_3; t) = 0, \quad \forall (x_1, x_2, x_3; t) \in \partial\Omega \times \mathbb{R}^+ \quad (68)$$

In (67), α_1 and α_2 are positive parameters destined to modulate the $x_1 - x_2$ period of the flow.

We shall perform a direct numerical solution of this flow by means of a solver developed by Orszag & Patera [21]. It is based upon space discretization in Fourier series in the $x_1 - x_2$ variables, and in series of Chebysev polinomials in the x_3 variable. In particular the velocity field is expanded as follows:

$$U(x_1, x_2, x_3; t) = \sum_{|n| \leq N} \sum_{|m| \leq M} v_{nm}(x_3, t) e^{i(\alpha_1 n x_1 + \alpha_2 m x_2)}, \quad (69)$$

with

$$v_{nm}(x_3, t) = \sum_{p=0}^P v_{nmp}(t) T_p(x_3).$$

Here, $T_p(x_3)$ is the p -th Chebysev polynomial, defined by $T_p(\cos\theta) = \cos(p\theta)$. Also N, M and P are given positive integer numbers.

This kind of discretization presents a special interest in our case. Indeed, it is possible to define initializations with two space scales for the Navier-Stokes equations (66). Given an integer number $L \leq \min(N, M)$, a positive number \hat{q}_0 , and a function $v : [0, 2\pi] \rightarrow \mathbb{R}^3$, we shall set $\epsilon = \frac{1}{L}$, and define

$$\left. \begin{aligned} U(x, 0) &= u_0(x_3) + \epsilon^{1/3} \sqrt{\hat{q}_0} \tilde{w}^0\left(\frac{x}{\epsilon}, x\right), \\ \text{with} \\ u_0(x_3) &= (x_3(2 - x_3), 0, 0), \quad \tilde{w}^0(y, x) = \tilde{w}^0(y_1, y_2; x_3) = 2\text{Re}[v(x_3)e^{i(\alpha_1 y_1 + \alpha_2 y_2)}]. \end{aligned} \right\} \quad (70)$$

Note that $u_0(x_3)$ is the basic parabolic profile associated to Poiseuille flow. Also, function v is normalized in such a way that \tilde{w}^0 has unit mean (in the x_3 variable) kinetic energy:

$$\frac{1}{2} \int_0^2 \frac{1}{2} \langle |\tilde{w}^0|^2 \rangle dx_3 = \frac{1}{2} \int_0^2 \langle |v(x_3)|^2 \rangle dx_3 = 1. \quad (71)$$

As a consequence, the initial mean kinetic energy is \hat{q}_0 .

The choice of function $v(x_3)$ is not arbitrary, as initialization (70) still has to verify two conditions imposed by the nature of the problem we are dealing with. Indeed, well-posedness of Navier-Stokes equations (66) requires $\nabla \cdot U(x, 0) = 0$. Also, the homogeneous boundary conditions (68) force v to be zero at the walls. These two restrictions cannot be verified unless

$$v_3(x_3) = 0 \quad \forall x_3 \in [0, 2],$$

due to the hypotheses of separation of scales. This leads to the discouraging conclusion that the y -helicity of \tilde{w}_0 must be zero. Nevertheless, this difficulty can be overcome for each fixed value of ϵ if we let \tilde{w}_0 depend also on ϵ . In practice, we have made the following choice for the function v :

$$\left. \begin{aligned} v &= \lambda_\epsilon (\epsilon v_1^*, v_2^*, v_3^*), \quad \text{with} \\ v_1^*(\xi) &= \begin{cases} (1+i)\xi(1-\xi) & \text{if } \xi \in [0, 1[, \\ (1+i)(1-\xi) & \text{if } \xi \in [1, 2]; \end{cases} \\ v_2^*(\xi) &= 2v_1^*(\xi); \\ v_3^*(\xi) &= \int_0^\xi [\alpha_1 v_1^*(\xi) + \alpha_2 v_2^*(\xi)] d\xi. \end{aligned} \right\} \quad (72)$$

Here, λ_ϵ is a normalization parameter, chosen in order to fit the normalization condition (71). In fact, λ_ϵ depends upon ϵ , but $\lambda_\epsilon = O(1)$ as $\epsilon \downarrow 0$.

We give in Figures 1, 2 and 3 a graphical description of the initial velocity field $U(x, 0)$. Figure 1 represents a general view of the initial mean velocity. Figure 2 represents the level lines of $U_1(x, 0)$ on the plane $z = \frac{3}{4}$. Here, the microstructures beared by $U(x, 0)$

can be observed. Also, figure 3 represents the sharp oscillations of $U_1(x, 0)$ on the straight line $y = \frac{\alpha_1}{2}\pi$, $z = \frac{3}{4}$.

In the sequel, we shall consider the flow described by equations (66)-(68) with the initial conditions given by (70) and (72). Note that this initialization does not fulfill completely the hypotheses of our theory, as it depends upon ϵ . Consequently, our test are meaningful only to test quantitative predictions for each fixed value of ϵ .

Let us now focus our attention on the practical aspects of our experiments. To test our model, we need to define computable equivalents \hat{u}^* of the mean velocity u , \hat{q}^* of the kinetic energy q , and \hat{h}^* of the helicity h . These parameters must be computed from the numerical solution of Navier-Stokes equations (66). To do this, we have considered as "microstructures" all harmonics of the flow associated to wavenumbers above a certain lower limit I . For instance, we have computed \hat{q}^* as the sum of energies corresponding to all wavenumbers (n, m) in (69) such that $I \leq |n| \leq N$, $I \leq |m| \leq M$:

$$\hat{q}^*(x_3, t) = \epsilon^{-2/3} \sum_{I \leq |n| \leq N} \sum_{I \leq |m| \leq M} |v_{nm}(x_3, t)|^2.$$

Also, the mean velocity field $\hat{u}^*(x, t)$ appears in practice to be very close to the one-dimensional velocity field $(v_{00}(x_3, t), 0, 0)$ for short times and relatively large levels of initial mean kinetic energy (Up to one half of the energy of u_0). Thus, we may assume

$$\hat{u}^*(x, t) = (v_{00}(x_3), 0, 0)$$

The calculation of the helicity \hat{h}^* is more laborious. Indeed, it involves the computation of the differential operator $\tilde{\nabla}_y = G \nabla_y$. As the mean flow is assumed to be one-dimensional, one obtains:

$$G = \nabla a = \begin{bmatrix} 1 & 0 & 0 \\ 0 & 1 & 0 \\ \alpha^* & 0 & 1 \end{bmatrix}, \quad \tilde{\nabla}_y = \begin{bmatrix} \frac{\partial}{\partial y_1} \\ \frac{\partial}{\partial y_2} \\ \alpha^* \frac{\partial}{\partial y_1} + \frac{\partial}{\partial y_3} \end{bmatrix};$$

where the parameter α^* is a function of x_3 and t , defined as follows:

$$\alpha_{,t}^* + \hat{u}_{1,3}^* = 0 \quad \text{for } (x_3, t) \in]0, 2[\times \mathbb{R}^+; \quad \alpha^*(x_3, 0) = 0 \quad \text{for } x_3 \in [0, 2]. \quad (73)$$

Moreover, we need a formal interpretation of the action of $\tilde{\nabla}_y$ on the expansion (69). What we have done is to take derivatives about the x variables; but assuming that the perturbation does not depend on x_3 . This interpretation leads to

$$\begin{aligned} \hat{h}^*(x_3, t) = & 2 \epsilon^{1/3} \operatorname{Re} \sum_{I \leq |n| \leq N} \sum_{I \leq |m| \leq M} i \left[(\alpha_2 m v_{nm}^{(3)} - \alpha^* \alpha_1 v_{nm}^{(2)}) \bar{v}_{nm}^{(1)} + \right. \\ & \left. + \alpha_1 n (\alpha^* v_{nm}^{(1)} - v_{nm}^{(3)}) \bar{v}_{nm}^{(2)} + (\alpha_1 n v_{nm}^{(2)} - \alpha_2 m v_{nm}^{(1)}) \bar{v}_{nm}^{(3)} \right]. \end{aligned}$$

Here, the superscripts indicate the components, the bar stands for complex conjugation, and the symbol “ i ” represents the complex number $\sqrt{-1}$. Note that, in particular,

$$\hat{h}^*(x_3, 0) = \langle \tilde{w}^0 \cdot \nabla_y \times \tilde{w}^0 \rangle .$$

In our experiments, the choice of the parameters ϵ , L , M and N is particularly important. Indeed, as time increases from zero, a double transfer of energy takes place from the wavenumber $n = m = L$ towards smaller and larger wavenumbers. Thus, a good spatial resolution of all small scales requires

$$1 \ll I \ll L \ll \min(N, M).$$

Moreover, we need to take L as large as possible in order to make the flow fit inside the asymptotic regime of our theory. In our test, we have given the following values to these parameters:

$$\left. \begin{aligned} L = 5, \quad I = 4, \quad N = M = 8 & \quad \left(\epsilon = \frac{1}{5} \right) \\ L = 10, \quad I = 5, \quad N = M = 16 & \quad \left(\epsilon = \frac{1}{10} \right) \\ L = 20, \quad I = 8, \quad N = M = 32 & \quad \left(\epsilon = \frac{1}{20} \right). \end{aligned} \right\}$$

Also, we have taken $P = 32$ in order to have a good resolution near the walls. The values of the other parameters is rather arbitrary. We have taken $\alpha_1 = \alpha_2 = 1.32$, in (67) and a inverse Reynolds number ν of order ϵ^2 . A typical value is $\nu = \frac{1}{500}$. Let us also remark that time steps have to be taken very small, as our flows are very rapidly oscillating. Typically, we have taken time steps ranging from 10^{-2} to 10^{-3} .

8.2 Numerical simulation with model equations

Let us now turn our attention to the description of the simulation of 3D Poiseuille flow between flat plates that we have performed by means of the model. In order to take into account eddy viscosity, and also for practical reasons, we shall consider a modified version of model (60), as follows:

$$\left. \begin{aligned} \text{(a)} \quad & u_{,t} + (u \cdot \nabla)u - \nu_a \Delta u + \nabla p = -\epsilon^{2/3} \nabla \cdot (q \hat{\mathbf{R}}) + \nu_t \epsilon^{4/3} \nabla \cdot [\sqrt{q}(\nabla u + \nabla u^T)], \\ \text{(b)} \quad & \nabla \cdot u = 0, \\ \text{(c)} \quad & a_{,t} + (u \cdot \nabla)a = 0, \quad a(x, 0) = x, \\ \text{(d)} \quad & q_{,t} + (u \cdot \nabla)q + q[\hat{\mathbf{R}} : \nabla u + \mu \hat{\psi}_q] = 0, \\ \text{(e)} \quad & h_{,t} + (u \cdot \nabla)h + h[\hat{\mathbf{S}} : \nabla u + \mu \hat{\psi}_h] = 0. \end{aligned} \right\} \quad (74)$$

Here, for simplicity of notation we have denoted

$$\hat{\mathbf{R}} = \hat{\mathbf{R}}(G) = G^{-T} \tilde{\mathbf{R}}^*(C) G^{-1}, \quad \hat{\mathbf{S}} = \hat{\mathbf{S}}(G) = G^{-t} \tilde{\mathbf{S}}^*(C) G^{-1},$$

$$\hat{\psi}_q = \hat{\psi}_q \left(C, \frac{h}{q} \right) = \left(\frac{h}{q} \right)^2 \psi_q^*(C), \quad \hat{\psi}_h = \hat{\psi}_h \left(C, \frac{h}{q} \right) = \left(\frac{h}{q} \right)^2 \psi_h^*(C).$$

Equation (74a) is equation (61) modified by including an artificial viscosity term $(-\nu_a \Delta u)$, in order to adapt the Navier-Stokes solver of Orszag & Patera. We have denoted here the mean velocity field by u instead of \bar{u}^ϵ , in order to simplify the notation. The value of the eddy viscosity coefficient in (74a) is $\nu_t = \frac{4}{9}$ (cf. [8]). Also, equations (74c), (74d) and (74e) are the corresponding ones for a , q and h in (60), where the mean velocity field has been replaced by the u of equation (74a). Thus equations (74c), (74d) and (74e) are accurate only up to order $\epsilon^{2/3}$. Note also that all variables u , a , q and h appear coupled in (74).

We shall use model (74) to compute the mean velocity field associated to the 3D Poiseuille flow described in Subsection 8.1. Then, the initial conditions for (74) must be

$$\left. \begin{aligned} u(x, 0) &= (u_0(x_3), 0, 0); \\ a(x, 0) &= x; \\ q(x, 0) &= q_0(x_3) = \hat{q}_0 |v(x_3)|^2; \\ h(x, 0) &= h_0(x_3) = 4\hat{q}_0 \text{Im}[(\alpha_2 v_1 - \alpha_1 v_2) \bar{v}_3]. \end{aligned} \right\} \quad (75)$$

Also, the boundary conditions for the mean velocity field u must be the same as those for the total velocity field, given by (67), (68). Moreover, a , q and h must be periodic in the x_1 and x_2 directions. No boundary condition in the x_3 variable is needed for a , q and h , as all of them verify transport equations driven by the mean velocity field, which is zero on the walls $x_3 = 0$ and $x_3 = 2$.

With these initial and boundary conditions, the solution of (74) is approximately one-dimensional for short times. To see this, let us consider the following system of PDE:

$$\left. \begin{aligned} \text{(a)} \quad & \tilde{u}_{1,t} + (\tilde{q} \hat{\mathbf{R}}_{13}(\alpha))_{,\xi} = 0, \\ \text{(b)} \quad & \alpha_{,t} + \tilde{u}_{1,\xi} = 0, \\ \text{(c)} \quad & \tilde{q}_{,t} + \tilde{q}(\hat{\mathbf{R}}_{13}(\alpha) u_{1,\xi} + \mu \hat{\psi}_q) = 0, \\ \text{(d)} \quad & \tilde{h}_{,t} + \tilde{h}(\hat{\mathbf{S}}_{13}(\alpha) u_{1,\xi} + \mu \hat{\psi}_h) = 0, \end{aligned} \right\} \text{for } (\xi, t) \in]0, 2[\times \mathbb{R}^+,$$

with initial and boundary conditions given by

$$\left. \begin{aligned} \text{(e)} \quad & \left\{ \begin{aligned} \tilde{u}_1(\xi, 0) &= u_0(\xi); \\ \alpha(\xi, 0) &= 0; \\ \tilde{q}(\xi, 0) &= q_0(\xi); \\ \tilde{h}_0(\xi, 0) &= h_0(\xi), \end{aligned} \right\} \text{for } \xi \in [0, 2], \\ \text{(f)} \quad & \tilde{u}_1(\xi, t) = \tilde{q}(\xi, t) = \tilde{h}(\xi, t) = 0, \quad \text{for } \xi = 0, 2; \quad t \geq 0. \end{aligned} \right\} \quad (76)$$

To every solution of this system there correspond a solution of the inviscid model equations (74) (i.e., $\nu_t = \nu_a = 0$), verifying the boundary and initial conditions described

above. This solution is given by

$$\left. \begin{aligned} u(x, t) &= (\tilde{u}_1(x_3, t), 0, 0); \\ q(x, t) &= \tilde{q}(x_3, t); \\ h(x, t) &= \tilde{h}(x_3, t). \end{aligned} \right\} \quad (77)$$

As viscous effects take a relatively long time to take place, we may assume that the mean flow is one-dimensional for short times. This will have consequences of practical relevance for our purposes, as we shall see in the sequel.

Let us now give an outline of the numerical methods used to solve model (74). To solve numerically equations (74d) and (74e) we have written both equations in logarithmic form. Let us focus our attention, for instance, in the equation for the helicity (74e). Let us define the variable z by

$$z = \log |h|,$$

in the regions where $h \neq 0$.

Then, z verifies

$$z_{,t} + (u \nabla) z + F = 0; \quad z(x_3, 0) = \log |h(x_3, 0)|,$$

with

$$F = \hat{\mathbf{R}} : \nabla u + \mu \hat{\psi}_h.$$

It is possible to recover h from z , as h cannot change sign along stream lines if it is continuous. This can be deduced from (74e). Indeed, if h vanishes in a point of a given stream line, then h must vanish on the whole flow line, as (74e) is proportional to h . In our case, the mean velocity is approximately given by (77) and then stream lines are straight lines parallel to the x_1 direction. Consequently, the helicity is given by

$$h(x, t) = h(x_3, 0) \exp\{z(x, t)\}.$$

Once written in logarithmic form, equation (74e) has been discretized in time by a Lax-Wendroff algorithm, as follows:

$$\left. \begin{aligned} z^{n+1} &= z^n - \Delta t (u^n \cdot \nabla z^n + F^n) + \frac{\Delta t^2}{2} u^n \cdot \nabla (u^n \cdot \nabla z^n + F^n); \\ h^{n+1} &= \text{sgn}(h^n) \exp\{z^{n+1}\}. \end{aligned} \right\} \quad (78)$$

This discretization is first-order accurate, and in practice bears good stability properties, because it includes decentered artificial viscosity.

Space discretization has been made by means of the mixed Fourier-Tchebycheff expansion (69) used by Orszag & Patera to discretize the velocity field. In particular, this kind

of discretization is very well suited to represent the large gradients of the function z in the x_3 variable near the walls.

Also, equation (74d) for the kinetic energy has been solved in the same way. In this case, the logarithmic formulation allows to keep non-negative the kinetic energy.

Velocity equations (74a)-(74b) have been discretized by means of an adaptation of the Orszag & Patera's solver. This adaptation consists in discretizing all terms coming from turbulence modelling (the right hand side of (74a)) with an explicit Adams-Bashforth second-order algorithm. At each time step, we have computed an intermediate velocity \hat{u}^n by

$$\left. \begin{aligned} \text{(a)} \quad & \frac{\hat{u}^n - u^n}{\Delta t} = \frac{3}{2} H^n - \frac{1}{2} H^{n-1} \\ \text{with} \\ \text{(b)} \quad & H^n = -\epsilon^{2/3} \nabla \cdot (q^n \hat{\mathbf{R}}^n) + \nu_t \epsilon^{4/3} \nabla \cdot [\sqrt{q^n} (\nabla u^n + (\nabla u^n)^T)]. \end{aligned} \right\} \quad (79)$$

Then, we have used \hat{u}^n as starting velocity to compute u^{n+1} with Orszag & Patera's solver.

Finally, equation (74c) for the Lagrangian coordinates has been discretized in time with a Lax-Wendroff scheme, similar to (78) with $F = 0$.

To complete the implementation of one time step, we still need to calculate the closure terms $\hat{\mathbf{R}}$, $\hat{\psi}_q$, $\hat{\mathbf{S}}$ and $\hat{\psi}_h$. We have tried to directly use the values issued from the tabulation of Ortegón in [23]. Unfortunately, these tabulations present very high gradients, that cause explosive instabilities in short time in our code. To solve this problem, we have replaced these values by analytic approximations as follows:

$$\left. \begin{aligned} \hat{\mathbf{R}}(G) &= \frac{2}{3} \frac{\text{Tr}(\bar{C})}{\bar{C} : \bar{C}} \bar{C}, \quad \bar{C} = G G^t; \quad \hat{\mathbf{S}}(G) = \hat{\mathbf{R}}(G); \\ \hat{\psi}_q(G) &= 7.5[\text{Tr}(\bar{C}) - 3]^2, \quad \hat{\psi}_h(G) = \hat{\psi}_q(G). \end{aligned} \right\} \quad (80)$$

These approximation roughly reproduce the qualitative behaviour of the computed closure terms as functions of the invariants of C , in what concerns growing and asymptotic behaviour at infinity.

To finish our description of the numerical solution of model (74), let us give some comments about the values of the parameters of numerical relevance. Typically, we have set the value of the artificial viscosity coefficient ν_a to be 1/4000, which is very small compared to velocities of order one, and seems to affect very slightly the value of the mean velocity field. Also, time steps have been taken relatively large, typically 10^{-1} , because the inclusion of eddy viscosity increases largely the stability of Orszag & Patera solver, when applied to solve the mean velocity equations (74a)-(74b).

As we have mentioned, the purpose of our experiments is to compare the solution (u, q, h) of model system (74) with initial conditions (75), with the quantities $(\hat{u}^*, \hat{q}^*, \hat{h}^*)$

issued from the solution of Navier-Stokes equations (66)-(68). In practice, u appears to be very close to \hat{u}^* as time increases, while there is a significant level of turbulent kinetic energy. Figures 4 to 7 represent the time evolution of \hat{q}^* and \hat{h}^* versus q and h , respectively for $\epsilon = \frac{1}{10}$. A fairly good agreement is found in the evolution of both quantities, in what concerns rate of decay and also transient effects. Our model fails to predict some transient features in the evolution of kinetic energy, for relatively large times. Analogous experiments corresponding to some other values of ϵ ($\epsilon = \frac{1}{5}$, $\epsilon = \frac{1}{20}$) result in a similar agreement.

9 Oscillatory behaviour of the transport of helical microstructures

As was pointed out already, our MPP models do not take into account turbulent diffusion. In fact, if we assume that the velocity u^c vanishes at infinity and we neglect viscous dissipation, then the total kinetic energy is conserved up to order $\epsilon^{4/3}$:

$$\frac{\partial}{\partial t} \int_{\mathbb{R}^3} \left(\frac{1}{2} |u + \epsilon^{2/3} \bar{u}^{(1)}|^2 + \epsilon^{2/3} q \right) dx = O(\epsilon^{4/3}).$$

This fact was analyzed in [6, 7] in the case of nonhelical microstructures; for the same kind of Poiseuille flow that we are considering here. It was found that the interaction large-small structures produces a certain oscillatory character of the mean flow, that could be explained by the MPP model.

This paragraph is devoted to stress that this is still the situation when the microstructures are helical. Indeed, Figures 8 and 9, that represent the rates of decay of kinetic energy and helicity, respectively, show a clear oscillatory character. This character has been found in many other simulations, for different values of ϵ and different initial levels of energy.

Our model equations can explain this fact, from a qualitative point of view. If viscous dissipation is neglected, then the mean flow described by model (60) is one-dimensional, and (60) reduces to

$$\left. \begin{aligned} \text{(a)} \quad & q_{,t} + q \hat{\mathbf{R}}_{13}(\alpha) \bar{u}_{1,\xi} = 0; \\ \text{(b)} \quad & \alpha_{,t} + \bar{u}_{1,\xi} = 0; \\ \text{(c)} \quad & h_{,t} + h \hat{\mathbf{S}}_{13}(\alpha) \bar{u}_{1,\xi} = 0; \\ \text{(d)} \quad & \bar{u}_{1,t}^{(1)} + (q \hat{\mathbf{R}}_{13}(\alpha))_{,\xi} = 0, \end{aligned} \right\} \quad (81)$$

This can be proved by means of an analysis similar to that applied in Section 8 to model (74). Then, the equation for h decouples from those for velocity and kinetic energy; and we retrieve the situation of nonhelical microstructures (cf. [6]). Now, starting from (81a)

and (81d) it is possible by linearization at $t = 0$ to derive a linear second order equation for the variable

$$v(\xi, t) = \int_0^t \bar{u}_1^{(1)}(\xi, s) ds. \quad (82)$$

This equation reads as follows (cf. [6, 19]):

$$v_{,tt} - \hat{q}_0 \lambda v_{,\xi\xi} = 0, \quad \lambda = \left. \frac{\partial \hat{\mathbf{R}}_{13}}{\partial \alpha} \right|_{\alpha=0}; \quad (83)$$

where q is assumed to take the constant value $\hat{q}_0 > 0$ at $t = 0$.

Numerical tabulations made in [22, 23] show that $\lambda > 0$, and then equation (83) is a wave equation. Consequently, our model predicts an oscillatory behaviour in the interaction large-small structures, in the case of 3D flows with one dimensional mean and helical microstructures.

Qualitatively, our numerical results agree with this prediction. However, quantitative predictions deduced from (83) do not agree with our numerical results. In particular, the dependency upon \hat{q}_0 of the period of the oscillations found in our experiments is different from the one that could correspond to (83). We think that this lack of agreement may be explained by the dependency upon ϵ of the function $w^0(y, x)$ we are taking.

As a conclusion, we can state that our model predicts reasonably well turbulent flows in two scales with helical microstructures. This result has to be added to preceeding simulations made in order to validate the same kind of flow with nonhelical microstructures. Both seem to support the conclusion that the MPP analysis models reasonably well locally homogeneous turbulence with two space scales.

Acknowledgements: The authors wish to thank Prof. O. Pironneau for his useful discussions and comments about this work, Prof. A. Patera for letting them use his Fortran codes, and also the French I.N.R.I.A., and in particular the MENUSIN Project, for its valuable computing facilities and scientific assistance.

References

- [1] G.K.BATCHELOR: *The Theory of Homogeneous Turbulence*.
Cambridge Univ. Press, Cambridge (1953).
- [2] C.BEGUE, B.CARDOT, O.PIRONNEAU: *Simulation of Turbulence with transient mean*.
International Journal for Numerical Methods in Fluids, Vol. 11, pp. 677-695 (1990).
- [3] C.BEGUE, T.CHACÓN, D.MCLAUGHLIN, G.PAPANICOLAOU, O.PIRONNEAU: *Convection of Microstructure, (II)*
Proc. 5th Int. Conf. In Numerical Methods in Engineering, Versailles 1983, (pp. 595-605), North Holland, Amsterdam (1985).
- [4] A.BEIRAO DA VEIGA: *Existence and asymptotic behaviour for strong solutions of the Navier-Stokes equations on the whole space*.
Indiana Univ. Jour., 36, pp. 149-166 (1987).
- [5] B.CARDOT: *Modélisation de la Turbulence par des Méthodes de Type $k - \epsilon$ et homogénéisation*.
Thèse de Doctorat, Université Paris VI (1986).
- [6] T.CHACÓN: *Oscillations due to the transport of Microstructures*.
SIAM J. Appl. Math. 48, pp. 1128-1146 (1988).
- [7] T.CHACÓN: *Étude d'un Modèle pour la Convection des Microstructures*.
Thèse 3^{ème} Cycle, Université Paris VI (1985).
- [8] T.CHACÓN: *Contribución al estudio del modelo MPP de turbulencia*.
Ph. D. Thesis, Univ. de Sevilla, Spain (1984).
- [9] P.G.CIARLET: *Elasticité Tridimensionnelle*.
Masson, Paris (1986).
- [10] P.G.CIARLET, J.M.THOMAS: *Introduction a l'Analyse Numérique Matricielle et à l'Optimisation*.
Masson, Paris (1982).

- [11] Y.COEFFE: *Les Modèles de Turbulence $k - \epsilon$ Appliqués à l'Écoulement Plan*.
EDF Report LNII HE 041/80.04 (1980).
- [12] C.CORDUNEANU: *Almost-periodic functions*.
Interscience Publishers, New York (1968).
- [13] D.FRANCO: *Una Versión Isótropa del Modelo MPP de Turbulencia*.
Graduation Thesis, Univ. Sevilla, Spain (1990).
- [14] F.HECHT, O.PIRONNEAU: *3D FE Simulation of Turbulent Flows around Vehicles*.
In "Computational Fluid Dynamic and Reacting Gas Flow". IMA Series, Vol. 12, pp.
69-89. Springer-Verlag, New York (1988).
- [15] O.A.LADYZHENSKAYA: *The Mathematical Theory of Viscous Incompressible Flows*.
Golden & Breach, New York (1969).
- [16] B.E.LAUNDER, D.B.SPALDING: *Mathematical Models of Turbulence*.
Academic Press, London (1972).
- [17] A.LEONARD: *Energy Cascade in Large-Eddy Simulations of Turbulent Fluid Flows*.
Adv. Geophys. 18a, pp.237-248 (1974).
- [18] J.L.LIONS: *Quelques Méthodes de Resolution des Problèmes aux Limites non
Linéaires*.
Dunod, Paris (1969).
- [19] D.MCCLAUGHLIN, G.PAPANICOLAOU, O.PIRONNEAU: *Transport of Microstructures
and Related Problems*.
SIAM J. Appl. Math. Vol. 45, N^o 5 (1985).
- [20] A.S.MONIN, A.M.YAGLOM: *Statistical Fluid Mechanics of Turbulence*.
Vol. 1 and 2, MIT Press, Cambridge (1975).
- [21] S.ORSZAG, A.PATERA: *Secondary Instability of Wall-Bounded Shear Flows*.
Jour. Fluid. Mech. 128, pp. 347-385, 1983.
- [22] F.ORTEGÓN: *Estudio de un modelo matemático de Turbulencia obtenido mediante
técnicas de Homogeneización*.
Ph. D. Thesis, Univ. Sevilla, Spain (1988).

- [23] F. ORTEGÓN: *Modélisation des écoulements turbulents à deux échelles par méthode d'Homogénéisation*.
Ph. D. Thesis, Univ. Paris VI (1989).
- [24] O. PIRONNEAU: *Numerical Modelling of Turbulent Flows with Two Scales*.
Journal de Mec. Teor. et Appl. N^o Special, pp. 95-107 (1986).
- [25] A. POUQUET, U. FRISCH, J.P. CHOLLET: *Flow with a Spectral Gap*.
Phys. Fluids, 26(4), pp. 877-880 (1983).
- [26] W.C. REYNOLDS: *Computations of Turbulent Flows*.
Am. Rev, Fluid. Mech. 8, pp.183-208 (1975).
- [27] W.C. REYNOLDS: *Physical and Analytical Foundations Concepts, and New Directions in Turbulence Modelling and Simulation*.
Proceedings "Ecole d'Eté CEA-EDF-INRIA d'Analyse Numérique-Modélisation Théorique de la Turbulence", Clamart, France (1982).
- [28] CH.G. SPEZIALE: *On Nonlinear $k - \epsilon$ and $k - l$ Models of Turbulence*.
J. Fluid. Mech., vol. 178, pp.459-475 (1987).
- [29] CH.G. SPEZIALE: *Turbulence Modelling in Nonlinear Frames of Reference*.
ICASE Report No. 88-18 (1988).
- [30] R. TEMAM: *Navier-Stokes Equations*.
North Holland, Amsterdam (1977).
- [31] S. ZAIDMAN: *Almost-periodic functions in abstract spaces*.
Research Notes in Mathematics, 126, Pitman, London (1985).

Captions to the figures.

Figure 1: Initial mean velocity field with parabolic profile for 3D Poiseuille flow between flat plates, corresponding to the numerical experiments described in Sections 8 and 9.

Figures 2: Typical level lines of the first component of the initial velocity on the plane $z = \frac{3}{4}$, corresponding to the numerical experiments described in Sections 8 and 9. The small structures can be clearly observed.

Figures 3: Profile of the first component of the initial velocity on the straight line $z = \frac{3}{4}, y = \frac{\alpha_1}{2}\pi$, corresponding to the numerical experiments described in Sections 8 and 9. Sharp oscillations can be observed.

Figures 4, 5, 6 and 7: Time evolution of physical kinetic energy $\epsilon^{2/3}\hat{q}^*$ (fig.4) and helicity $\epsilon^{-1/3}\hat{h}^*$ (fig.6), computed from direct solution of 3D Poiseuille flow (66)-(67) versus kinetic energy $\epsilon^{2/3}q$ (fig.5) and helicity $\epsilon^{-1/3}h$ (fig.7), computed from solution of model equations (74).

Both simulations correspond to $\epsilon = \frac{1}{10}$, $\Re = 500$, $\epsilon^{2/3}\hat{q}_0 = 0.1$, with closure terms given by (80). The artificial viscosity in (71) is $\nu_a = \frac{1}{4000}$.

Figures 8 and 9: Rate of decay of mean turbulent kinetic energy and helicity, for $\epsilon = \frac{1}{5}$ and $\epsilon = \frac{1}{10}$, respectively. An oscillatory behaviour predicted by our model is clearly made apparent.

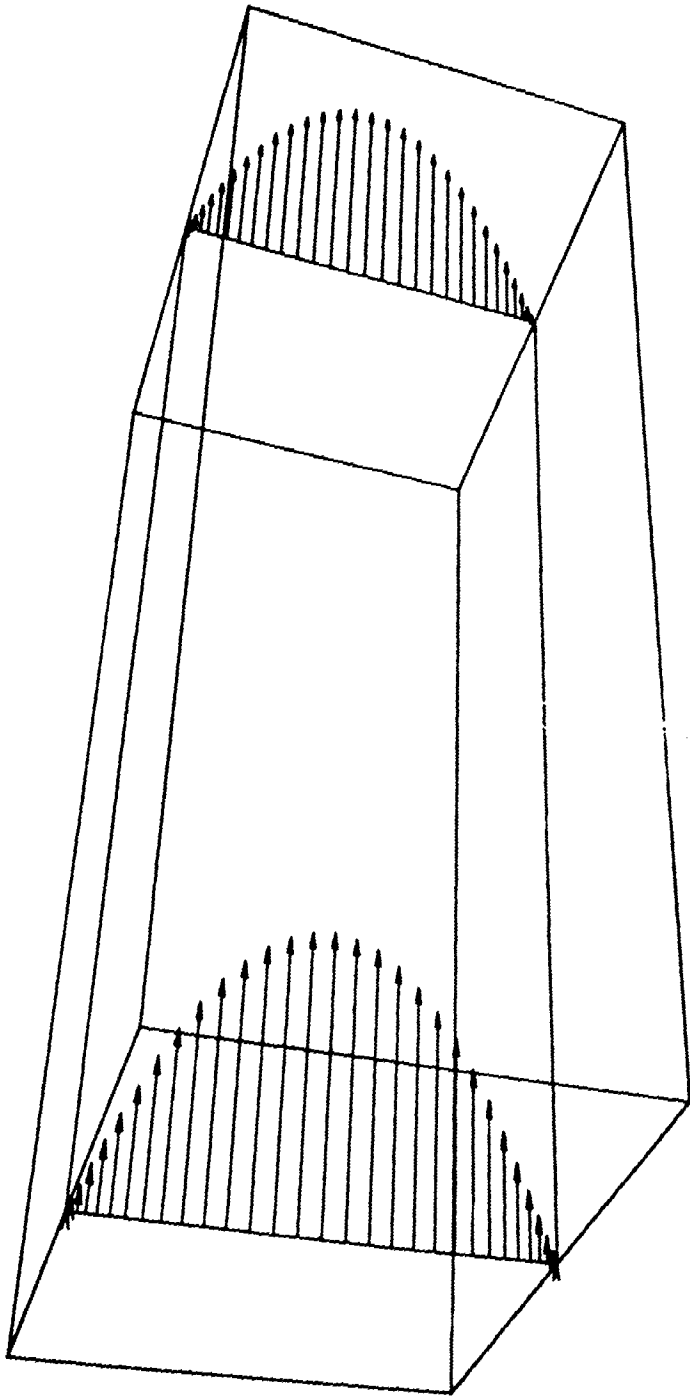


Figure 1

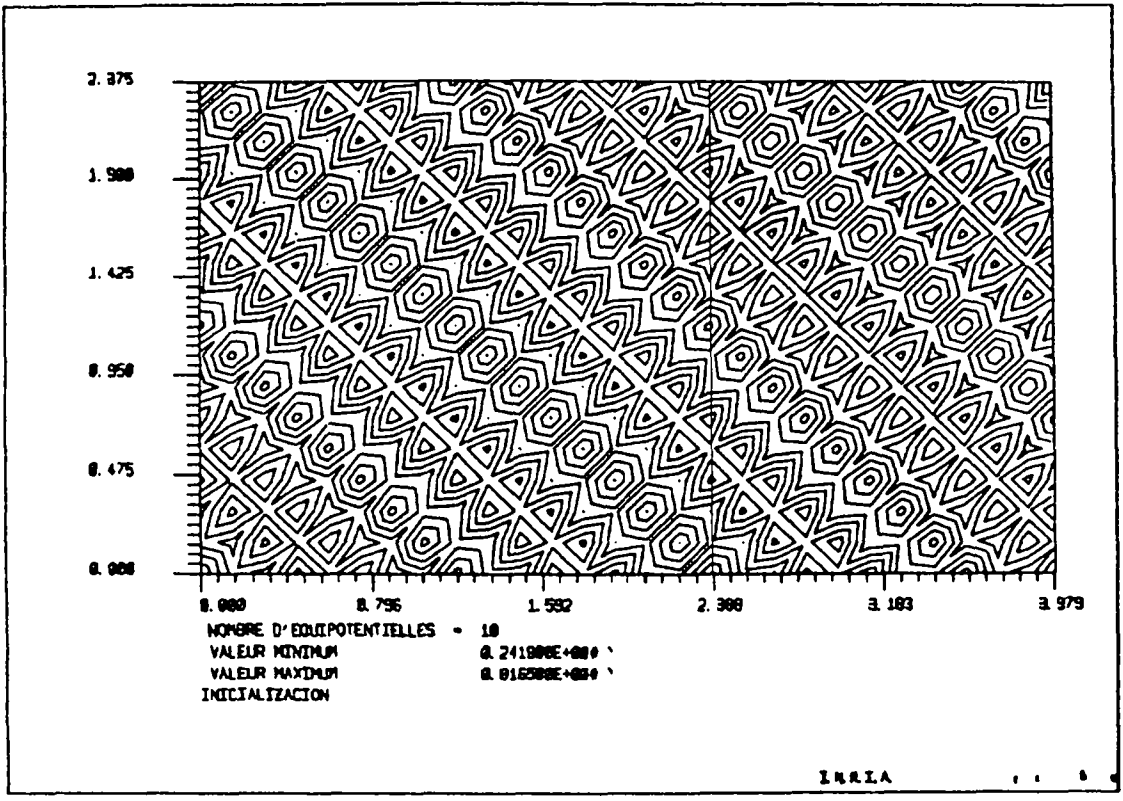


Figure 2

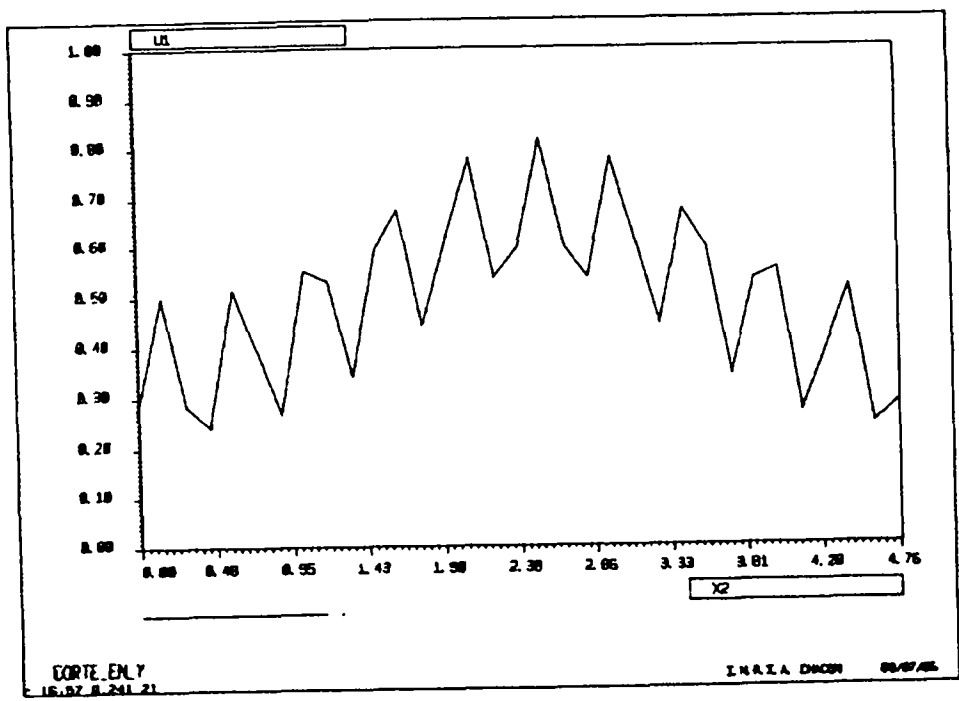
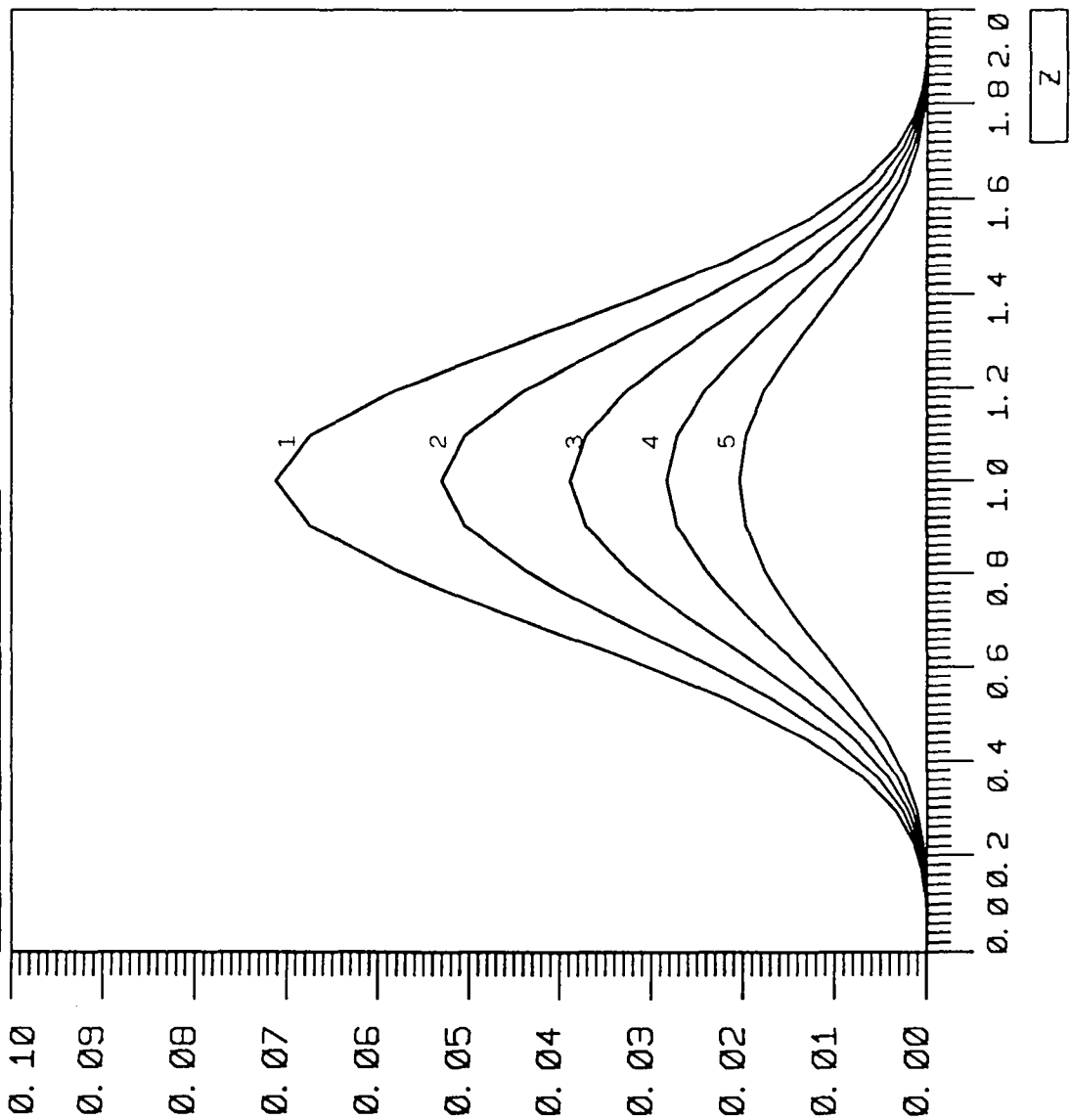


Figure 3

KINETIC ENERGY



MODULEF : ortegon

01/08/89

qpat.le10.lhel

NOMBRE DE COURBES : 5

EXTREMA EN X :

0.00 2.0

EXTREMA EN Y :

0.00 0.71E-01

- 1 : T = 0
- 2 : T = 0.2
- 3 : T = 0.4
- 4 : T = 0.6
- 5 : T = 0.8

TRACE DE COURBES

Figure 4

MODULEF :	ortegon
01/08/89	
q1010	
NOMBRE DE COURBES :	5
EXTREMA EN X :	
0.00	2.0
EXTREMA EN Y :	
0.00	0.71E-01
—	1 : T = 0
—	2 : T = .2
—	3 : T = .4
—	4 : T = .6
—	5 : T = .8
TRACE DE COURBES	

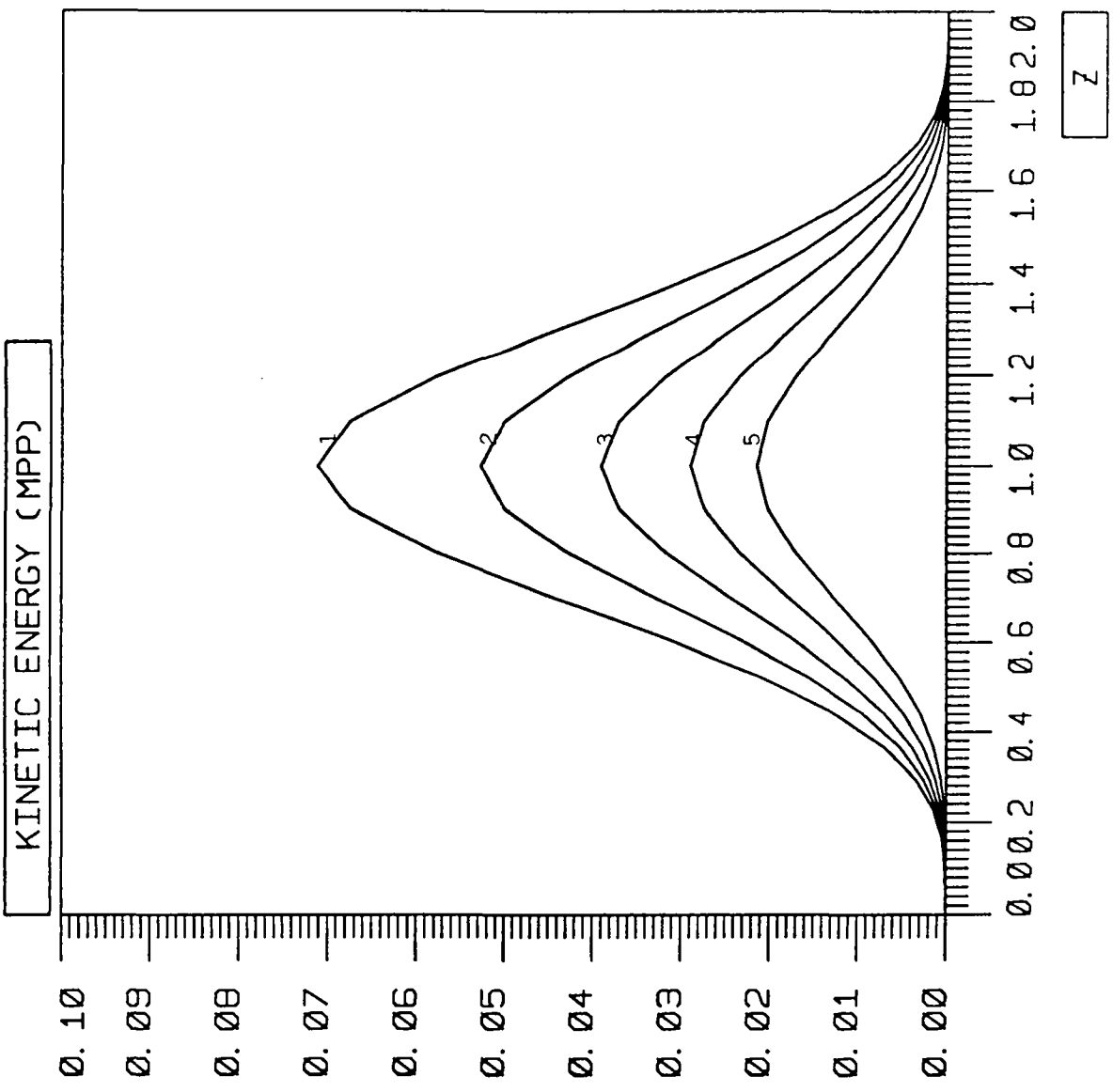


Figure 5

MODULEF : ortegon

01/08/89

hpat1010

NOMBRE DE COURBES : 5

EXTREMA EN X :

0.00 2.0

EXTREMA EN Y :

-0.93E-01 0.93E-01

1 : T = 0

2 : T = 0.2

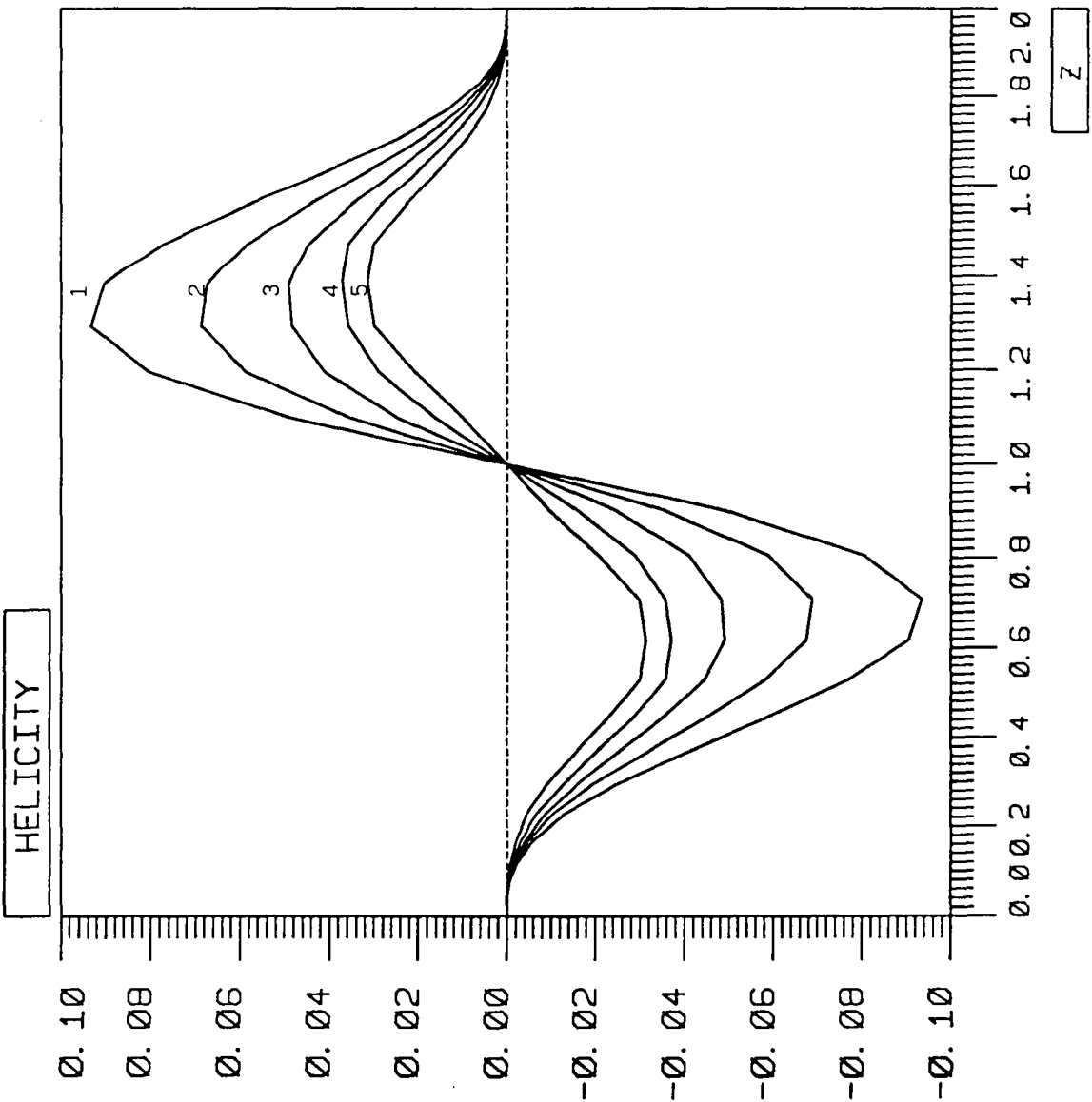
3 : T = 0.4

4 : T = 0.6

5 : T = 0.8

TRACE DE COURBES

Figure 6



MODULEE : ortegon

01/08/89

h1010

NOMBRE DE COURBES : 5

EXTREMA EN X :

0.00 2.0

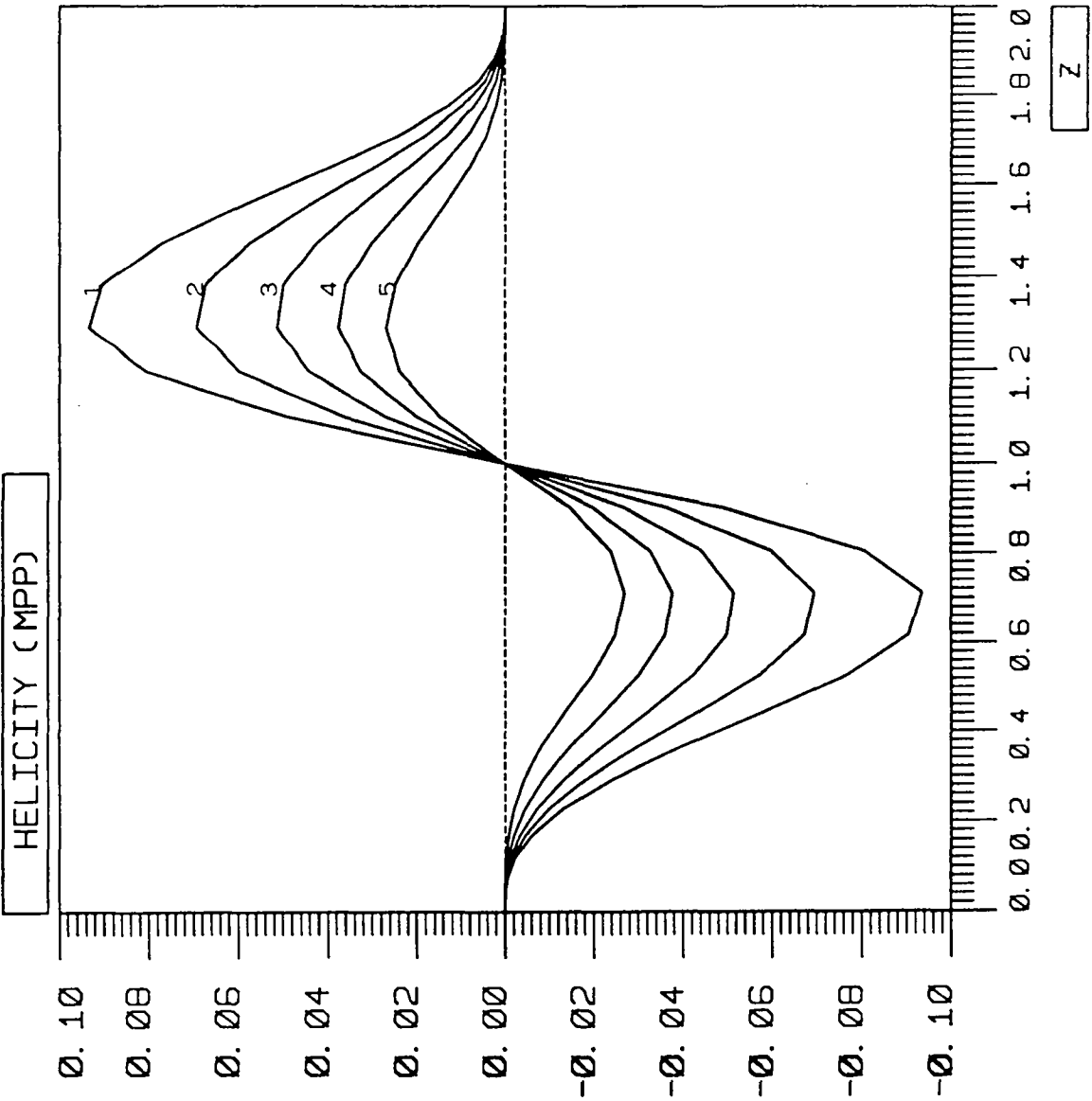
EXTREMA EN Y :

-0.93E-01 0.93E-01

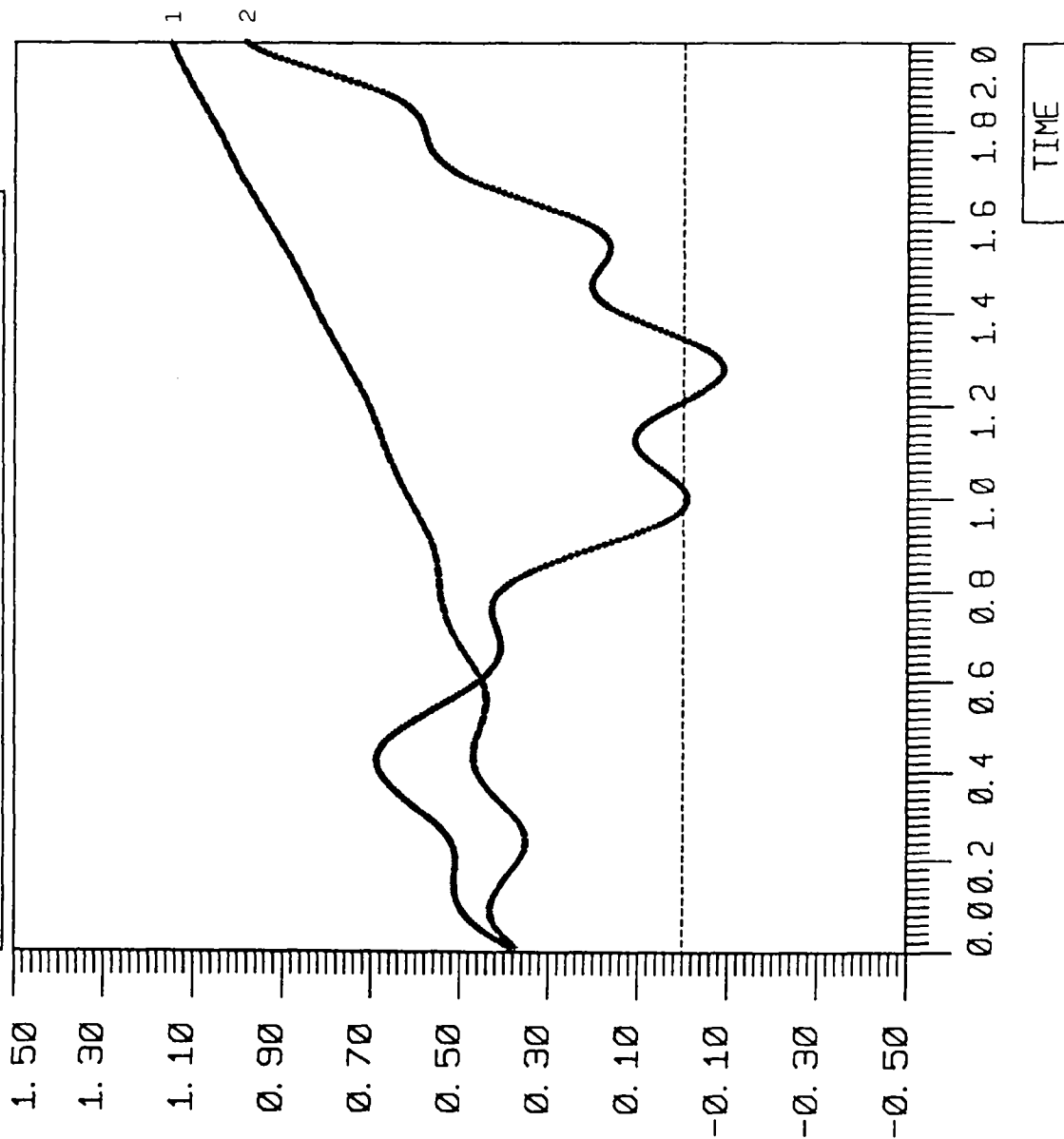
1 : T = 0
2 : T = 0.2
3 : T = 0.4
4 : T = 0.6
5 : T = 0.8

TRACE DE COURBES

Figure 7



DISSIPATION RATES, EPS = 1/5



MODULEF : ortegon

24/08/89

taxhq.5.1

NOMBRE DE COURBES : 2

EXTREMA EN X :

0.10E-01 2.0

EXTREMA EN Y :

-0.89E-01 1.2

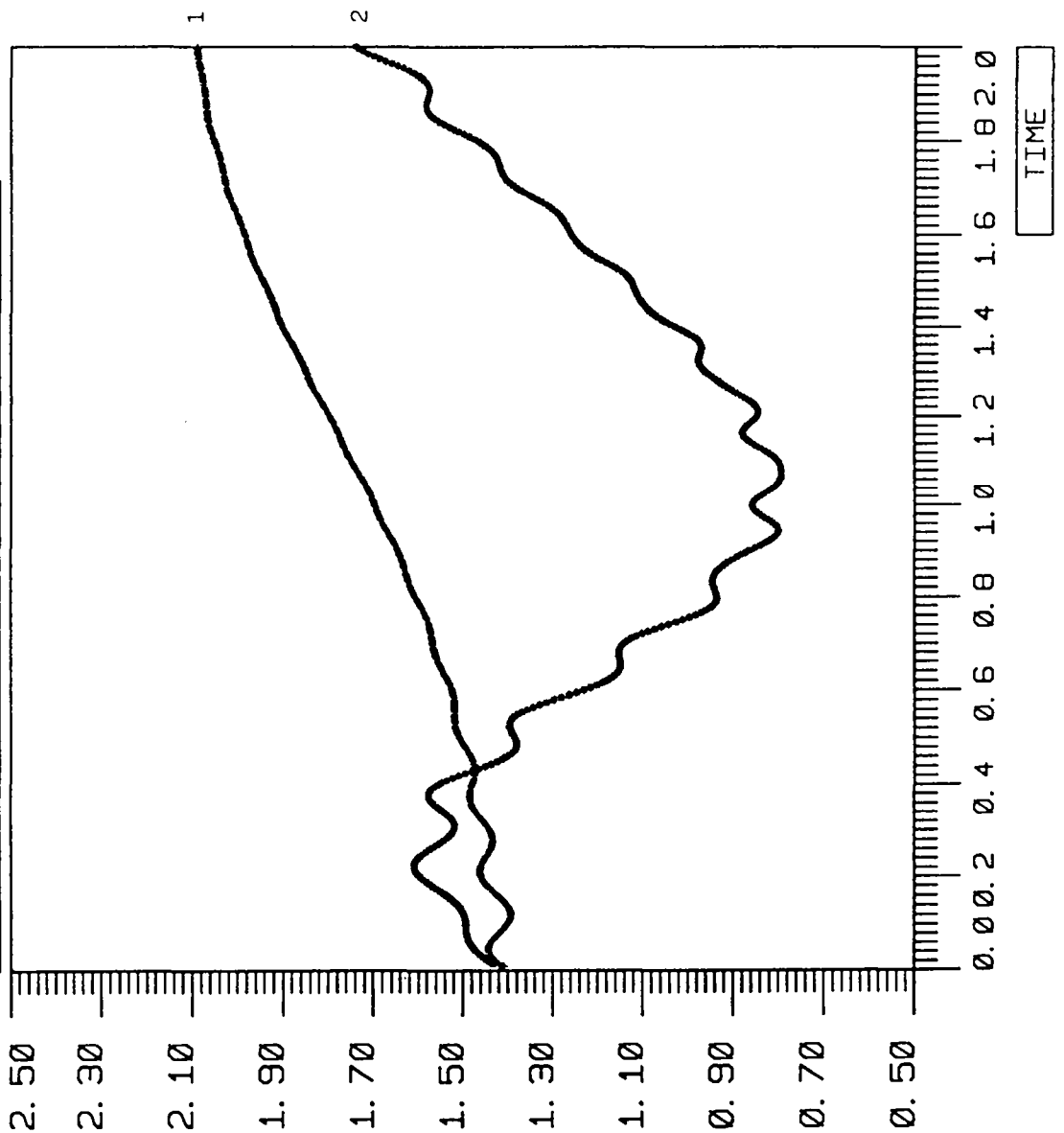
* * * 1 : HELICITY

* * * 2 : KINETIC ENERGY

TRACE DE COURBES

Figure 8

DISSIPATION RATES, EPS = 1/10



MODULEF : ortegon

24/08/89

taxhq.10.1

NOMBRE DE COURBES : 2

EXTREMA EN X :

0.10E-01 2.0

EXTREMA EN Y :

0.79 2.1

* * * 1 : HELICITY

* * * 2 : KINETIC ENERGY

TRACE DE COURBES

Figure 9

ISSN 0249-6399